Journal Pre-proofs

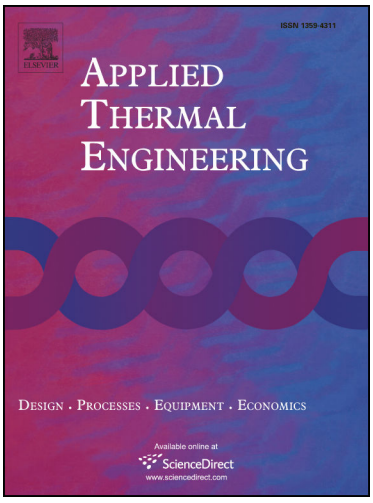

Research Paper

Modelling and analysis of a compression/resorption heat pump system with a zeotropic mixture of Acetone/CO_2

Paúl Dávila, Mahmoud Bourouis, Juan Francisco Nicolalde, Javier Martínez-Gómez

PII: S1359-4311(23)00417-9
DOI: https://doi.org/10.1016/j.applthermaleng.2023.120388
Reference: ATE 120388

To appear in: *Applied Thermal Engineering*

Received Date: 22 November 2022
Revised Date: 3 March 2023
Accepted Date: 9 March 2023

Please cite this article as: P. Dávila, M. Bourouis, J. Francisco Nicolalde, J. Martínez-Gómez, Modelling and analysis of a compression/resorption heat pump system with a zeotropic mixture of Acetone/CO_2, *Applied Thermal Engineering* (2023), doi: https://doi.org/10.1016/j.applthermaleng.2023.120388

Modelling and analysis of a compression/resorption heat pump system with a zeotropic mixture of Acetone/CO_2

Paúl Dávila[12], Mahmoud Bourouis[2], Juan Francisco Nicolalde[13*], Javier Martínez-Gómez[345]

1 Escuela de Ingeniería Industrial, Universidad Internacional Del Ecuador, Quito 170411, Ecuador. padavilaal@uide.edu.ec (P.D), junicolaldego@uide.edu.ec (J.F.N)
[2] Departamento de Ingeniería Mecánica, Universitat Rovira i Virgili, Tarragona 43007, España. mahmoud.bourouis@urv.cat (M.B)
[3] Facultad de Ingeniería y Ciencias Aplicadas, Universidad Internacional SEK, Quito 170302, Ecuador; javier.martinez@uisek.edu.ec (J.M-G)
[4]Instituto de Investigación Geológico y Energético (IIGE), Quito 170518, Ecuador
[5]Universidad de Alcalá, Departamento de teoría de la señal y comunicación, (Área de Ingeniería Mecánica) Escuela Politécnica, 28805 Alcalá de Henares, Madrid, España
Corresponding: junicolaldego@uide.edu.ec

Abstract: Industrial processes represent one of the most energy-consuming activities, which are related to fossil fuel utilization and the growing environmental problems. In this way, the heat waste energy recovery has been presented as an efficient solution, to take advantage of low-grade residual heat, where the compressor -resorption heat pump technology has proven to achieve high-temperature levels with a considerable Coefficient of Performance. However, known working fluids such as hydrofluorocarbons represents an environmental hazard due to its Global Warming potential, these have been replaced by natural fluids such as ammonia, but they also have disadvantages like its toxicity. In this way, the CO_2 is an available waste heat compound product of fossil combustions, therefore, this research is based on the utilization of novel fluids such as the zeotropic mixture of CO_2/Acetone as an eco-friendly working fluid with low Global Warming Potential. Even more, the utilization of the mentioned compound represents the opportunity to explore the utilization of low-grade residual heat that sometimes is not used in subsequent applications. In this sense, the modelling of the binary vapor-liquid equilibria of the mixture CO_2/Acetone has been performed based on a thermodynamic model using the Peng-Robinson equation regarding the conditions of pressure, temperature, and concentration of the fluids for operational industry applications. The modelling of the compression/resorption heat pump cycle is based on the mass and energy balance for each component with Engineering Equation Solver software (EES). In this way, the adjustment of equilibria for the mixture determinates the maximum average square deviation of 4.28 % and 8.70 % for a temperature range between 291 to 303 K and 333 to 393 K. The concentration of CO_2 from 20 % to 50 % showed that the increasing molar fraction delivers a more efficient cycle, even reaching a coefficient of performance of 3 for a difference of 0.2 between the global concentration of CO_2 and the poor solution, and a 20 ºC temperature difference between source and sink. Even more, the COP obtained in the simulation was not affected by variations of steam mass flow rate and it was proven that the mathematical model proposed has a correlation with the literature.
Keywords: compression, resorption; heat pump; zeotropic mixture; Peng-Robinson; waste heat

Nomenclature

Acronyms

PR	Peng-Robinson
VLE	Vapor-Liquid Equilibrium

Subscripts

w	Acentric factor of Pitzer
P_{crit}	Critical Pressure
T_{crit}	Critical Temperature
Z	Compressibility Factor
ρ	Density
h	Enthalpy
R	Ideal gas constant
l	Liquid phase
ṁ	Mass Flow
x	Molar fraction on liquid phase
y	Molar fraction on vapour phase
V_m	Molar volume
MW	Molecular weight
m	Parameter in the function of acentric factor of Pitzer

α	Parameter in the function of reduced temperature
C	Peneloux correction factor
P	Pressure
T_R	Reduced Temperature
T	Temperature
$\emptyset$	Transience of the phase
v	Vapour phase

Nomenclature

$cal \times mol^{-1} \times K^{-1}$	Constant coefficient of gases
$kg \times m^{-3}$	Density
$KJ \times Kg^{-1}$	Enthalpy
$KJ \times Kg^{-1} \times K^{-1}$	*Entropy*
$J \times mol^{-1} \times K$	*Ideal gas Constant*
$kg \times s^{-1}$	Mass flow
$g \times mol^{-1}$	Molecular weight
$cm^3 \times gmol^{-1}$	Molar volume
Bar	Pressure
˚K/˚C	Temperature
$cm^3 \times gmol^{-1}$	Vapour molar volume

1. Introduction

Regarding the global energy consumption that has as the main source the utilization of fossil fuels, the problems related to energy and the environment has become prominent, where, the industrial processes in China represents one of the most consuming energy activity, having a 71,1% share of the primary energy consumption [1]. Even more, regarding the heating needs in the building and industry sectors, 75 % of the final energy is used for this purpose, and in European countries such as the Netherlands, the chemical and refinery industries produce over 100 PJ of waste energy per year, facts that make consider that more efficient use of waste energy could have a major effect on energy consumption and therefore carbon footprint [2]. In this sense, as an industrial heat waste recovery solution heat pumps have improved the energy efficiency of industrial processes by taking advantage of the low-grade waste heat recovery [3]. Whereas high-temperature heat pumps as an alternative for enhancing energy efficiency have reached large temperature lifts over 80 °C [4] making it a technology that within its reaches can also provide space heating [5] and consequently contribute as a solution for energy and environmental pollution problems [6]. Furthermore, research to improve the efficiency of thermal systems has been developed by experimenting with different refrigerants to analyse the thermodynamic behaviour of the operation parameters [7]. In this sense, the heat pumps technology has advanced and classified as mechanical heat pumps and absorption heat pumps (AHP), where, the first type uses high Global Warming Potential (GWP) refrigerants, while the AHP that works with eco-friendly fluids [3] is based on a vapour-absorption cycle [8], and agrees with the international protocols implemented to reduce the greenhouse gases in the atmosphere [9]. Even more, the heat pumps can also reduce the energy consumption since its development has reached different industrial applications [10]. In this sense, considering the worldwide interest in solving problems such as global warming, heat pump technologies offers a practical solution to offset the greenhouse emissions by recirculating the environment and waste heat from the industrial processes [11]. In this way, it has been studied the different industrial sector that produces useful heat, such as the production of paper, food, chemicals, automotive, metal, textile, wood, and other, where it has been found that processes release temperatures between the 20°C and 200°C [12] , therefore, the heat pump technology has been catalogued as a heating capacity increasing system, efficient and stable [13].

In this sense, the AHP has been used with several heat sources such as exhaust gases, gas burners, and solar power among others, where the utilization of this heat has been applied to space heating, water heating, drying, industrial pre-heating and industrial distillation [14]. However, this technology is

limited by the thermodynamic behaviour of the working fluids and the resistance of its components to reach elevated temperatures useful in industrial processes. Nevertheless, the absorption heat pumps cannot provide temperature lifts, and in this way, resorption systems are considered an alternative to the conventional vapour compression pumps. Even more, an advantage of this technology is the compatibility to use environmental friendly refrigerants such as water, ammonia and CO_2 [15]. In this sense, traditional heat pump systems are composed by a compressor, expansion valve and a condenser, but a compressor resorption heat pump (CRHP) has a resorber-desorber instead of a condenser and evaporator, allowing to achieve high-temperature levels with relatively good Coefficient Of Performance (COP) [16], that are enhanced by the application of these hybrid systems [17]. Since the absorption-resorption is a non-isothermal process where the entropy generation decreases regarding the temperature difference [18], the relevance of a high COP responds to the fact that only if this is greater or equal to the energy factor of an electric generator, the heat pump could emit less carbon dioxide compared to the traditional heating systems [19]. In this sense, the CRHP also known as an absorption-resorption heat pump, has been described as a promising application when low temperature is used for space heating [20]. The interest in this system has grown in theoretical and experimental aspects, delivering successful implementations on commercial units [21], which is the typical application due to their large size [22]. Even more, this system has shown to be an appropriate alternative to the conventional heat pumps, considering that has limitations like the temperature of discharge in the compressor [23]. In this way, authors like Gudjonsdottir & Infante Ferreira [24], have concluded that the CRHP technologies are a clear option to upgrade waste heat streams. Moreover, the CRHP system can be found as an evaporator-condenser system that can be integrated with different heat sources such as waste heat, gas engine, Organic Rankine Cycle and microturbine, where the resorption subsystem can work with LiBr-H_2O, LiCl-H_2O and NH_3-H_2O and the compression subsystem may use R134a, R410A, NH_3, low- GWP HFO refrigerants and CO_2 [25]. On the other hand, the working pairs for desorption/resorption systems are fluids that consume or produce heat, with the benefits of having good thermal properties on the working conditions such as thermal storage, conductivity, stability heat transfer coefficient, along with other characteristics like non-corrosive, non-toxic, etc. [26].

However, some vapour-compression technologies use potent greenhouse gases refrigerants such as hydrofluorocarbons (HFC) but can be replaced by natural fluids that reduce the environmental impact. In this sense, the compression resorption systems can use zeotropic binary mixtures as a working fluid, that have the advantage that produces a reduction on vapour pressures compared to other volatile fluids [27]. Even more, zeotropic mixtures have important boiling temperature differences, whereas mixtures of ammonia-water have been studied but its toxicity has led to the research of other mixtures such as the carbon dioxide and ammonia mixture. In this way, the mixtures of ammonia-water has been studied on absorption-compression heat pumps, allowing to conclude that is a promising and efficient alternative on the utilization of high temperatures for industrial applications [27]. On the other hand, the CO_2-based zeotropic mixtures have drawn the attention in the field since it can integrate different benefits and enhance the Coefficient of performance of the system [28]. In this way, several studies that include numerical simulations as experimental proposals have shown results with increments on the COP by analysing the combinations of CO_2 and hydrocarbons [29]. Furthermore, regarding the superior performance of CO_2 as a supercritical fluid and the characteristics of being inexpensive, stable, abundant [30], and considering the low COP of vapour compression cycles using CO_2, experiments were carried out by circulating the CO_2 with a low volatile absorption liquid as a co-fluid [31]. In this way, CO_2 has been catalogued as a natural refrigerant with great potential for its environmental and thermodynamic characteristics on experimental research of transcritical heat pumping cycles [32]. In this sense, Groll & Kruse [33], proposed the utilization of acetone as the absorbent resulting in modelling with a good agreement with the experimental result [31], also, Mozurkewich et al [34], simulated a refrigeration cycle for a co-circulation and wet compression of CO_2 and absorbing co-fluids such as N-methyl-2-pyrrolidone, Neopentylglycol diacetate, γ-Butyrolactone and Acetone, concluding that the maximum theoretical COP is obtained when the entropy generation rate is minimized and the best mixture is CO_2-Acetone. Furthermore, when compared the miscibility of the CO_2 with other fluids such as toluene and monochlorobenzene in an analysis of pressure-density-temperature near critical states, the acetone proved to be the best for CO_2[35]. In this way, the carbon dioxide (CO_2) is a non-toxic compound that can be found as a gas in atmospheric conditions of 1bar and a temperature of 20°C,

and shares 0.03% of the atmospheric volume, while a liquid phase is present in a temperature range of -56.6°C to 31.1°C at a minimum pressure of 5.2 bar [36]. On the other hand, acetone is a solvent with a boiling and fusion temperature of 56.2°C and -95.4°C respectably, it has a solubility on the water of 0.791 $kg \times l^{-1}$ and vapour pressure of 0.24 Bar at 20°C [37].

The mixture of the CO_2/Acetone has been studied by several authors under different conditions, where the modelling of the binary vapour-liquid equilibria can be correlated by using the Peng-Robinson equation [38]. In this sense, the research of Han et al [39], showed an equilibrium of the vapour mixture on a pressure interval of 2.36 MPa to 11.77 MPa, a temperature between 333.15 K to 393.15 K and a molar fraction of CO2 of 0.32 to 0.92. In the thermodynamic diagram of equilibrium liquid-vapour of the binary mixtures of CO_2 with acetone and pentanes made by Hsieh & Vrabec, [40] the pressure studied was from 5.13MPa to 11.8MPa, temperatures of 313.15, 333 and 353 ˚K with a molar fraction of CO_2 of 0.48 to 0.85. On the other hand, the research of Chiu et al., [41] studied the isothermal vapour-liquid equilibrium (VLE) phase boundaries of the mixtures CO_2 with ethanol and CO_2 with acetone at temperatures from 291.15K to 313.15K with different compositions that include molar fractions of CO_2 from 0.19 to 0.98 for pressures from 0.72 MPa to 7.95 MPa, is important to point out that these investigations indicate that the acetone is an effective absorbent of CO_2 and has the best miscibility for CO_2 compared to other absorbents. Furthermore, in recent studies Ramírez-Ramos et al [42], proved that the CO_2 can show good miscibility and solubility with acetone at temperatures of 283.15K to 383.15K in a composition of 0.04 to 0.85 CO_2 mole fraction for pressure up to 8.7MPa, showing a steady VLE. On the other hand, regarding the modelling of the compression-absorption heat pump systems, several researchers have used computational methods to validate the thermodynamic processes in different models, these software uses an iterative procedure to solve equations and converge on a numerical solution [43]. In this sense, the research of Jensen et al [44], made a thermodynamic model of ammonia-water mixture on a compression-absorption heat pump system, calculating the properties of the mixture by software along with the transport properties, following the equations and correlations referenced in the literature. In this way, the simulation used an iteration of 50 steps for the desorber and the absorber, allowing to determinate the pitch point temperature differences [44]. On the other hand, Liu et al [45], used the Aspen plus software to study a mixture of a high-temperature CAHP waste heat recovery system and declared a COP with a relative error of 0.54% compared to the literature, meaning reliable results and useful information. In this way, this investigation proposes the study of the zeotropic mixture of Acetone-CO_2, considering the low GWP and its non-hazardous nature compared to other much more studied working fluids, to be used as an alternative eco-friendly working fluid for compression-resorption heat pump systems with low thermal energy, considering the lack of research on industrial applications. Furthermore, in the medium term this contribution can constitute a basis for the studies regarding the recovery of residual heat at low temperatures (40 to 60°C), and be able to produce a thermal repower at useful temperatures (80 to 120°C) for the same industry. Even more, regarding the bibliographical research and with aid of the Aspen software [46], the present research has the objective of modelling the behaviour of the mixture CO_2/Acetone following the Peng-Robinson equations considering the pressure, temperature, and concentration for the application of a CRHP on the industrial sector, meaning the simulation of an alternative working fluid. In this sense, this work establishes a parametric analysis for different operative conditions that allows obtaining a range of limitations to apply the binary mixture to the industry and opening the path for further experimental research based on the results obtained.

2. Method and Materials

The bibliographical research allowed to analyse the different methods that have been used to calculate the thermodynamic properties of the binary mixtures of Acetone/CO_2. In this sense, the authors has used the state equations of Soave Redlich Kwong, Patel-Teja and Peng-Robinson (PR) due to the mathematical relative simplicity [47]. In a general way, the PR equation shows better approximations between calculated data and experimental values, demonstrating lower deviations in the results presented. The researches of Hsieh & Vrabec, [40] and Han et al. [39], are part of the studies that

recommend the utilization of the state equation of PR to determine the VLE and other characteristics of the CO_2/acetone mixture, making this the chosen method to be used. The properties are determined so that the same properties can be used in the simulation of the compression/resorption heat pump cycle, to study the CO_2/acetone mixture as the working fluid for this type of cycle.

2.1. Thermodynamic properties model

The PR method allows to calculate of the VLE, enthalpy, entropy and density of the mixture, the state equation [47] is expressed in equations (1) to (5) as:

$$P = \frac{RT}{v-b} - \frac{a}{v(v+b)+b(v-b)} \quad (1)$$

Where:

$$a = 0.45724 \frac{R^2 T_{crit}^2}{P_{crit}} \alpha \quad (2)$$

$$b = 0.07780 \frac{RT_{crit}}{P_{crit}} \quad (3)$$

$$\sqrt{\alpha} = 1 + m(1 - \sqrt{T_r}) \quad (4)$$

$$m = 0.37464 + 1.54226w - 0.26992w^2 \quad (5)$$

2.2. Peng-Robinson equation for mixtures

The PR equation has been declared, however, for this research the fluid that will be studied is a compound of Acetone and CO_2. For this matter, the properties of the materials are displayed in table 1 and the PR equation for mixtures is expressed in equation (6), where the Pitzer's acentric factor (w) represents the spherical symmetry of the CO_2 and the acetone as a molecular force field [48]

Table 1. *Compound properties*[49]

Parameter	Unit	CO_2	Acetone
P_{crit}	bar	72.8	46.4
T_{crit}	K	304.2	508.1
v	$cm^3 x\ gmol^{-1}$	94	209
w	-	0.225	0.309
MW	$g\ x\ mol^{-1}$	44.01	58.08

$$P = \frac{RT}{(v - b_m)} - \frac{a_m}{v(v + b_m) + b_m(v - b_m)} \quad (6)$$

For the mixture of CO_2/Acetone it has been used the classic rules of Van der Waals (Klein) that describe the characteristic parameters of a_m and b_m as follows in equations (7)-(8):

$$a_m = a_1 x_1^2 + a_2 x_2^2 + 2 x_1 x_2 a_{12} \quad (7)$$

$$b_m = b_1 x_1^2 + b_2 x_2^2 + x_1 x_2 b_{12} \quad (8)$$

Corresponding the sub-index (1) to CO_2 and (2) for acetone, the interaction parameters a_{12}; b_{12} are calculated with equations (9)-(10), where k_{12} is the parameter of binary interaction of the mixture.

$$a_{12} = \sqrt{a_1 \times a_2} \times (1 - k_{12}) \quad (9)$$

$$b_{12} = \frac{1}{2}(b_1 + b_2) \quad (10)$$

Following the PR state equation in terms of the compressibility factor, equations (11)-(13) corresponds to a cubic formulation which resolution that has been taken from the book of thermodynamics by Klein & Nellis, 2011 [50] as follows:

$$Z^3 - (1-B)Z^2 + (A - 3B^2 - 2B)Z - (AB - B^2 - B^3) = 0 \quad (11)$$

$$A = \frac{a_m P}{R^2 T^2} \quad (12)$$

$$B = \frac{a_m P}{RT} \quad (13)$$

Likewise, the determination of the VLE along with other properties requires the parameter of binary interaction of the mixture in terms of temperature pressure and concentration, which are obtained from the adjustment of experimental data of the factor *K* that is calculated as $K=y \times x^{-1}$ from the previous studies of Han et al. [39], Hsieh & Vrabec [40], Chiu et al. [41] and Ramírez-Ramos et al. [42]. In this sense, for the mathematical iterative model based on PR the factor *K* can be calculated using the transience of each phase for every fluid as follows in equation (14):

$$K_i = \frac{\emptyset_i^l}{\emptyset_i^v} = \frac{l_i}{v_i} \quad (14)$$

The calculation of *K* must be compared and repeated with the initial K_i value until it has a tolerate proximity showing convergence in the value. Furthermore, the transience $\emptyset$ of the compound is calculated with equation (15), where the terms *AA* and *BB* corresponding to combination parameters are calculated with equations (16-17) and as follows.

$$\ln \emptyset_i = (BB)_i(Z_i - 1) - \ln(Z_i - B) - \frac{A}{2\sqrt{2B}}((AA)_i - (BB)_i)\ln\left[\frac{Z_i + (\sqrt{2}+1)B}{Z_i - (\sqrt{2}-1)B}\right] \quad (15)$$

$$(AA)_i = \frac{2}{\alpha a_m}\left[\sum_i^2 (a\alpha)_i\right] \quad (16)$$

$$(BB)_i = \frac{b_i}{b_m} \quad (17)$$

Furthermore, the transience of the compound in the liquid phase is calculated with equation (18), where the term $\emptyset^l_{i_{(T,P_{sat})}}$ refers to the transience of the compound in saturation conditions and V_l corresponds to the molar volume of a liquid phase. On the other hand, the transience of the component in the vapour phase is expressed by equation (19).

$$\emptyset^l_i = \emptyset^l_{i_{(T,P_{sat})}}{}^{\frac{v_l(p-P_{sat})}{RT}} \quad (18)$$

$$\ln\left(\frac{\emptyset^v_i}{P}\right) = Z_i - 1 - \ln(Z_i - B) - \frac{A}{2\sqrt{2B}}\ln\left[\frac{Z_i + (\sqrt{2}+1)B}{Z_i - (\sqrt{2}-1)B}\right] \quad (19)$$

Lastly, the cubic model equation of PR proposes the relation between the parameter of binary interaction with the temperature according to the following equation (20):

$$k_{12} = k_1 + k_2 T + \frac{k_3}{T} \quad (20)$$

The coefficients k_1, k_2 and k_3 were found using a modification in the objective function of the fit of the experimental data using the ASPEN PLUS software [46].

Furthermore, the PR model and the values of binary interaction for different temperatures allows to achieve a graphic of the vapour pressure of the CO_2/Acetone mixture in the function of the molar composition of CO_2. Moreover, the Duhring diagram (PTXY) shows the graph of vapour pressure versus temperature for different concentrations of CO_2 in the liquid phase and vapour phase of the CO_2 / Acetone mixture. The Clausius-Clapeyron equation states that when in a system formed by a pure substance or a mixture with two phases in equilibrium at a temperature T and a pressure P, a temperature change represents a change in pressure for the restoration of equilibrium thermodynamic [51]. In this

sense, assuming that the vapour phase is an ideal gas, and that the molar volume of the liquid is negligible compared to the molar volume of the vapour, the so-called Clausius-Clapeyron equation is reached, which describes the vapour pressure of the mixture as a function of temperature, considering an enthalpy of vaporization. The relationship between the change of both magnitudes is given in equation (21) where $\Delta H_{v\ represents}$ the molar enthalpy of vaporization and its integration under the assumption that ΔH_v is constant in the interval of temperature and pressure resulting in the equation (22).

$$\frac{d\ln P}{dT} = \frac{\Delta H_v}{RT^2} \quad (21)$$

$$\ln P = -\frac{\Delta H_v}{RT} + C \quad (22)$$

Considering ΔH_v as a constant, the graphical representation of $\ln P$ versus $1\times T^{-1}$ corresponds to a straight line with slope $-\Delta H_v \times R^{-1}$ [51].

Furthermore, the following figure 1 represents the logical sequential order that has been followed to determine the properties of the CO_2/acetone mixture. This scheme summarizes the procedure defined in points 2.1 and 2.2.

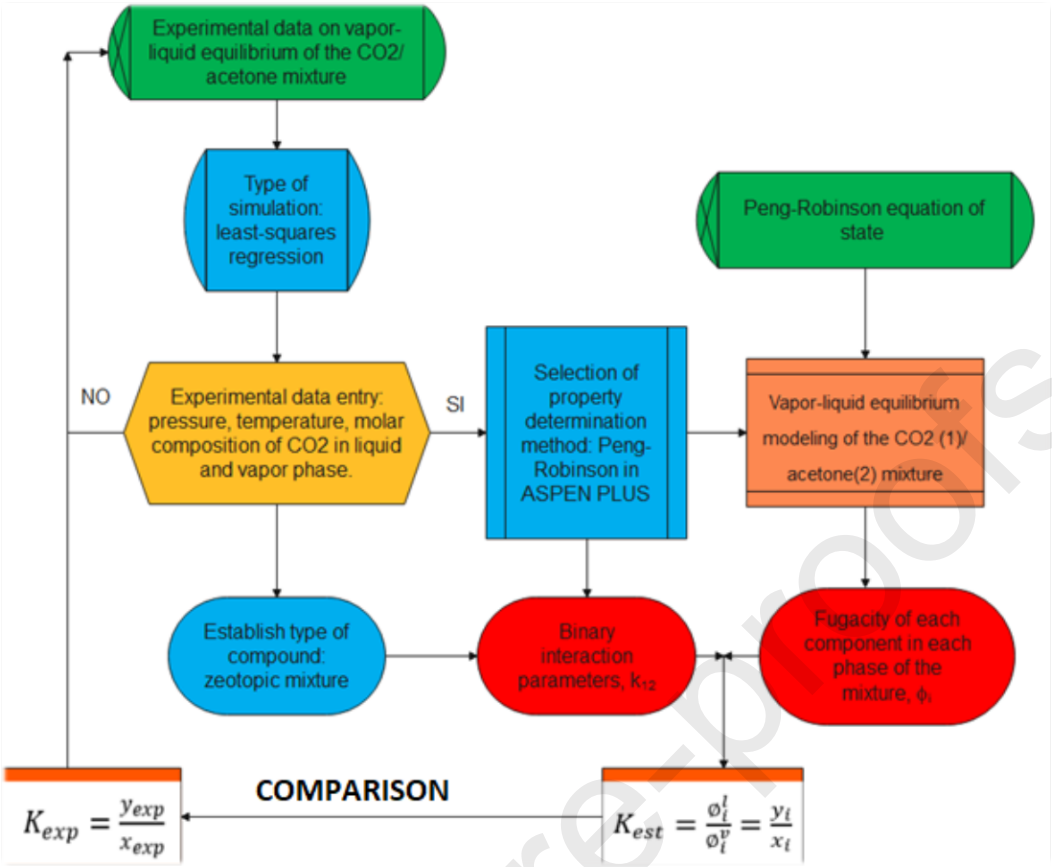

Figure 1. *Logical procedure for the determination of VLE properties of the CO2/acetone mixture*

2.3. Determination of Density of the mixture

Following the state equations, the density of the mixture CO_2/Acetone is determined in the liquid and vapor state. This density is obtained through the compressibility factor Z with the equation (23), where R is the constant of ideal gases with the value of R=8.314 J×mol^{-1}K^{-1}. This factor is calculated for each phase Z_l (liquid) and Z_v (vapor) with the equations (24-25) respectively.

$$Z = \frac{PV_m}{RT} \quad (23)$$

$$V_{ml} = \frac{Z_l RT}{P} = \frac{1}{\rho_l} \quad (24)$$

$$V_{mv} = \frac{Z_v RT}{P} = \frac{1}{\rho_v} \quad (25)$$

Furthermore, with the data expressed by Ramírez-Ramos et al., [42], a correlation between the density of the mixture in the liquid phase with the composition and the temperature is performed, obtaining the following equation (26) for the molar fraction of CO_2 in the CO_2/Acetone mixture (XCO_2) as a function of the temperature and the density. Where the terms T_n and ρ_n are expressed by equations (27) and (28)

$$X_{CO_2} = \rho_{00} + (\rho_{10} * T_n) + (\rho_{01} * \rho_n) + (\rho_{20} * {T_n}^2) + (\rho_{11} * T_n * \rho_n) + (\rho_{02} * {\rho_n}^2) \\ (\rho_{21} * \rho_n * {T_n}^2) + (\rho_{12} * T_n * {\rho_n}^2) + (\rho_{03} * {\rho_n}^3) \quad (26)$$

$$T_n = \frac{(T - 291.6)}{5.57} \quad (27)$$

$$\rho_n = \frac{(\rho - 864.8)}{34.59} \quad (28)$$

Density calculations with the Peng-Robinson equation have been improved using the specific volume correction factor proposed by Péneloux et al. [52] to the Soave-Redlich-Kwong (SRK) equation. The correction is specific to each substance and independent of temperature. The authors propose to generalize the constants used in the correction equation through the Rackett compressibility factor, ZRA. The Péneloux volume correction factor directly influences the calculation of the molar volume obtained by the Peng Robinson equation of state and is applied as shown by the equation (29) that calculates the molar volume correction for the liquid state (V_{mlcorr}) using the correction factor of Péneloux (C) that is expressed by equation (30), being C_i the specific correction coefficient for CO_2 (C_1) and acetone (C_2) that can be calculated by equation (31).

$$V_{ml_{corr}} = V_{ml} - C \quad (29)$$

$$C = \sum_{i}^{2} (X_i C_i) \quad (30)$$

$$C_i = 0.40768\frac{RT_{crit}}{P_{crit}}(0.29441 - Z_{RA_i}) \quad (31)$$

In this sense, the Rackett parameters for CO_2 (Z_{RA_1}) are 0.272 and for acetone (Z_{RA_2}) 0.244 [49]

2.4. Calculation of enthalpy and entropy of the mixture CO_2/Acetone

The enthalpy of the mixture (h) has been calculated from the enthalpy of the ideal mixture and the enthalpy of deviation of the mixture is obtained with the Peng-Robinson equation of state expressed in equation (32). In this way, the enthalpy of an ideal mixture ($h_{idealmix}$) is calculated with equation (33), which at the same time considers the ideal gas enthalpy of each component, which can be calculated from the ideal gas heat capacity, $C^o_{p_i}$ by integration as shown in equation (34).

$$h = h_{idealmix} - h_{dev} \quad (32)$$

$$h_{idealmix} = \sum_{i=1}^{2}(h_i * x_i) \quad (33)$$

$$h_i = \int C^o_{p_i} * dT \quad (34)$$

On the other hand, to directly calculate the ideal gas heat capacity of each component it has been used the expression presented by Fouad et al. [53] is displayed in equation (35), where, the expression *B, C, D, E, F* are constant coefficients for each component which are displayed in table 2.

$$C^o_{p_i} = B + C\left[\frac{(D/T)}{Sinh(D/T)}\right]^2 + E\left[\frac{(F/T)}{Cosh(F/T)}\right]^2 \quad (35)$$

Table 2. *Constants for CO2 and Acetone*

Coefficients	B $cal \times (molK)^{-1}$	C $cal \times (molK)^{-1}$	D K	E $cal \times (molK)^{-1}$	F K
CO_2 (1)	14.508	37.979	1709.8	24.296	799.14
Acetone (2)	7.5405	7.5162	1442.7	5.3802	647.50

Lastly, the expression of the deviation of enthalpy (h_{dev}) for the mixture is calculated using the following equation (36) described by Klein & Nellis [50], where the expression $B=b_mP\times(RT)^{-1}$ is the constant of the mixture as a characteristic parameter for the mix CO_2(1)/Acetone(2) and $\frac{da}{dT}$ refers to the variational output of enthalpy regards to T.

$$h_{dev} = R.T(1-Z) + \left(\frac{a_m - T\frac{da}{dT}}{2\sqrt{2}b_m}\right)\ln\left(\frac{Z+2.414B}{Z-0.414B}\right) \quad (36)$$

The entropy of the mixture (S) has been calculated from the entropy of the corrected ideal mixture, regarding the deviation of the mixture obtained with the Peng-Robinson equation (37). Hence, the entropy of the ideal mixture ($S_{idealmix}$) is calculated with equation (38). In this way, S_i represents the entropy of the ideal gas and X_i the molar fraction of component i in the mixture.

$$s = s_{idealmix} - s_{desv} \quad (36)$$

$$s_{idealmix} = \sum_{i=1}^{2}(s_i * x_i) \quad (37)$$

Furthermore, the ideal gas entropy of each component can be calculated in the same way from the ideal gas heat capacity ($C_{p_i}^o$) by integration according to expression (39) and the term deviation of entropy (S_{desv}) has been taken from the work of Klein & Nellis, [50] as shown in equation (40)

$$\mathrm{S_i} = \int\left(\frac{C_{p_i}^o}{T}\right) * dT \quad (38)$$

$$s_{desv} = -R.Ln(Z-B) - \left(\frac{1}{2\sqrt{2}b_m}\frac{da}{dT}\right)\ln\left(\frac{Z+2.414B}{Z-0.414B}\right) \quad (39)$$

The calculations of the entropy are as important as the enthalpy since these properties are needed for the calculation of mass and energy in the simulation of the heat pump.

2.5. Compression/resorption heat pump cycle simulation

Compression/resorption heat pump cycle simulation is a thermodynamic model based on the mass and energy balances for each component of the cycle, and on certain typical hypotheses in this type of cycle. In this sense, figure 2 shows a simplified scheme of the heat pump cycle that operates with the zeotropic mixture of CO_2/Acetone. The compression/resorption heat pump cycle is made up of a solution circuit and a vapour line. When using the zeotropic mixture (CO_2/Acetone) the stream leaving the desorber (stage 4) is a liquid/vapour mixture. This stream is separated at the desorber outlet in the component defined as "separator" so that the vapour phase stream is directed towards the compressor (stage 5) while the solution stream (stage 7) is driven by the solution pump to the resorber, previously the solution passes through the “hot” side of the solution heat exchanger, to increase the temperature of the solution (stage 8). On the other hand, the vapour stream from the compressor (stage 6) and the stream from the desorber (stage 9) meet in the component defined as “mixer”. The biphasic mixture enters the resorber (stage 10) where the absorption process is completed with heat dissipation in the sink and leaves the resorber (stage 11). This stream first passes through the solution heat exchanger, where it preheats the stream from the desorber, and then through the expansion valve (stage 12). The expansion valve (stage 3) causes a pressure drop in the circuit and consequently an increase in the temperature of the mixture. Finally, the biphasic solution enters the desorber again and completes the solution circuit.

Figure 2 shows a schematic of a compression/resorption heat pump cycle, consisting mainly of a resorption solution circuit (two-phase mixture) and a steam line. The evaporation of the zeotropic mixture in the desorber is not complete, the stream leaving the desorber is a liquid/vapor mixture. This stream is separated, the vapor phase is sent to a mechanically driven compressor while the liquid is recirculated to the resorber (comparable to the condenser in a compression cycle) via a solution pump. The main advantage of compression/resorption cycles involves the better performance due to pressure reduction compared to the compression case using pure refrigerant, and the improvement of cycle efficiency due to lower internal and external temperature gradients. in the desorber and reabsorb (Lorentz cycle). Furthermore, the heat production can be varied by changing the concentration of the solution flowing between the desorber and the resorber.

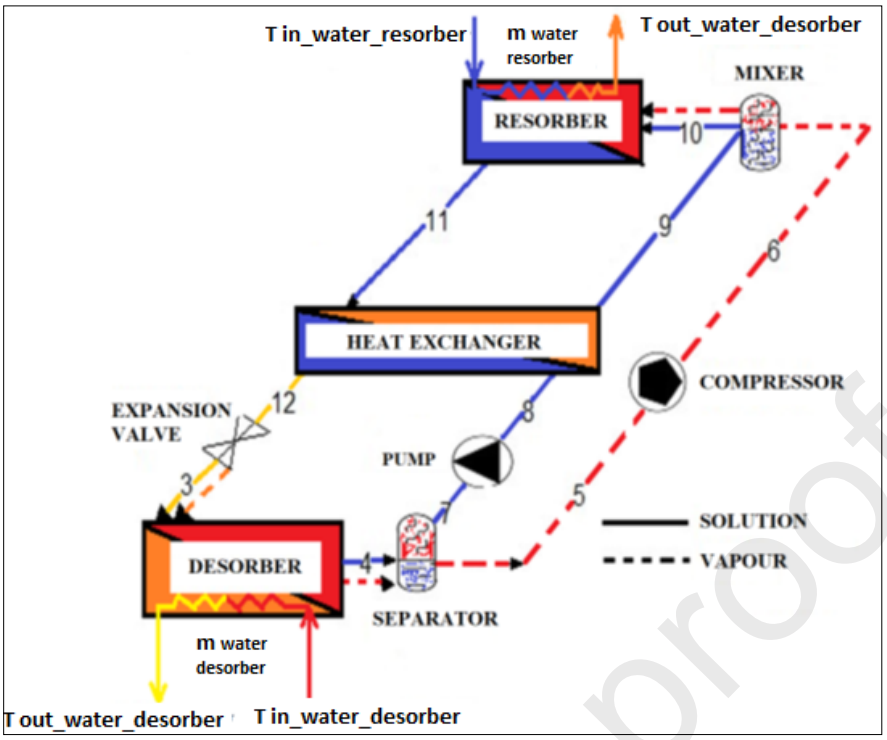

Figure 2. *Heat pump cycle*

The operating conditions of the compression/resorption heat pump cycle are defined by the operating range of its independent variables. The modelling of the cycle is based on the mass and energy balance for each component of the compression/resorption heat pump thermodynamic cycle and a series of conditions of the fluid states at the outlet or inlet of the components. In this sense, to determine these independent variables, it is necessary to show the logical sequence of resolution of the cycle, where table 3 shows the equations of the mass and energy balance for each component of the cycle and table 4 the hypotheses assumed for the operation of the compression/resorption heat pump cycle, being the subscript numbering of each point referred to the stages described in figure 2.

Table 3. *Mass and energy balances for each component in the modelling of the compression/resorption heat pump cycle using the CO2/acetone mixture.*

Component of the cycle	Balance equations
Desorber	• $m_{(3)} = m_{l(4)} + m_{v(4)}$ • $m_{(3)}.X_{(3)} = m_{l(4)}.X_{l(4)} + m_{v(4)}.X_{v(4)}$ • $m_{(3)}.h_{(3)} = m_{l(4)}.h_{l(4)} + m_{v(4)}.h_{v(4)}$ • $Q_{des} = m_{(3)} \times (h_{(4)} - h_{(3)})$
Separator	• $T_{(4)} = T_{(5)} = T_{(7)}$ • $X_{(7)} = X_{l(4)} = X_{(8)} = X_{(9)}$ • $X_{(5)} = X_{v(4)} = X_{v(6)}$

Pump	• $h_{l\,(8)} = h_{l\,(7)} + wp_1$ • $wp_1 = [1/\rho_{l\,(7)} \times (P_{high} - P_{low})]/\mathcal{E}_{pump}$ • $wp = wp_1 * m_{l\,(4)}$
Compressor	• $sy_{(6)} = sy_{(5)}$ • $w_{comp} = [m_{v\,(4)} \times (h_{Iin\,(6)} - h_{(5)})]/eff_{comp}$ • $h_{(6)} = h_{(5)} + w_{comp}/m_{v\,[4]}$
Heat exchanger	• $\mathcal{E}_{hex} = (T_{(9)} - T_{(8)})/(T_{(11)} - T_{(8)})$ • $\mathcal{E}_{hex} = Q_{real}/Q_{max}$ • $Q_{hex} = m_{l\,(4)} \times (h_{l\,(9)} - h_{l\,(8)})$ • $Q_{hex} = m_{(3)} \times (h_{l\,(11)} - h_{(12)})$
Mixer	• $m_{(10)} = m_{l\,(9)} + m_{v\,(6)}$ • $m_{(10)}.\, X_{(10)} = m_{l\,(9)}.\, X_{l\,(9)} + m_{v\,(6)}.\, X_{v\,(6)}$ • $m_{(10)}.\, h_{(10)} = m_{l\,(9)}.\, h_{l\,(9)} + m_{v\,(6)}.\, h_{v\,(6)}$
Resorber	• $h_{(10)} = (h_{l\,(9)} + (h_{v\,(6)} - h_{l\,(9)})) \times q_{(10)}$ • $m_{(11)} = m_{l\,(10)} + m_{v\,(10)}$ • $m_{(11)}.\, X_{(11)} = m_{l\,(10)}.\, X_{l\,(10)} + m_{v\,(10)}.\, X_{v\,(10)}$ • $m_{(11)}.\, h_{(11)} = m_{l\,(10)}.\, h_{l\,(10)} + m_{v\,(10)}.\, h_{v\,(10)}$ • $Q_{res} = m_{(10)} \times (h_{(10)} - h_{(11)})$
Expansion valve	For a biphasic mixture: • $h_{(3)} = (h_{l\,(3)} + (h_{v\,(3)} - h_{l\,(3)})) \times q_{(3)}$ • $h_{(3)} = h_{(12)}$

Furthermore, the simulation of the heat pump cycle is carried out in a sequential order that allows relating the mass and energy balance in each component, for which the Engineering Equation Solver (EES) software was used. The calculated values of the properties of the mixture in the liquid phase and vapour phase, along with the mass and energy balances in each component and the conditions assumed

by the model that are displayed in table 4. An ideal efficiency was used in the pump, compressor, heat exchanger and expansion valve to simplify the analysis of the cycle, with the focus of the present work on the behaviour of the CO_2/acetone mixture when it is used in the compression/resorption heat pump cycle. In addition, with these assumptions it is expected to obtain a database regarding the thermodynamic parameters (Pressure, temperature, and composition) in which the cycle using this mixture is functional.

Even more, for the simulation, the independent variables considered for the compression/resorption heat pump cycle using the CO_2/Acetone mixture are declared in table 5.

Table 4. *Hypothetic conditions*

Description	Assumed condition
Heat pump cycle	• Equilibrium in the biphasic mixture • Stages (3); (4); (10) $q=m_v/m_{total}$ • Saturation conditions: Stages (5); (7) (11) • Effectiveness of heat exchanger of the solution $\varepsilon_{hex=1}$ • Isentropic performance of the pump $\varepsilon_{pump}=1$ • Isentropic performance of compressor $\varepsilon_{comp}=1$ • Isenthalpic process in the expansion valve
External circuits	• $T_{out\_water\_resorber} - T_{in\_water\_resorber} = 5\ ^{\circ}C$ • $T_{in\_water\_desorber} - T_{out\_water\_desorber} = 5\ ^{\circ}C$

For the assumptions previously mentioned, isentropic performance in the pump and the effectiveness in the heat exchanger are justified in that the mathematical model applied for the simulation is reproducible and a feasible solution is obtained. For a more realistic simulation, both assumptions can be changed, and the cycle efficiency will decrease. However, it is important to mention that this work is intended to test whether the CO_2/acetone mixture is suitable for use in a compression/resorption heat pump.

In this way, Figure 3 shows the performance of the cycle under standard operating conditions. Here the following conditions are established as input conditions in the simulation: desorber outlet temperature of 30°C, resorber outlet temperature of 50°C, overall CO_2 molar concentration difference in the mixture of 0.10, high pressure of 40 bar and a steam mass flow rate of 1 $kg \times s^{-1}$. The results obtained were: a temperature difference between the inlet and outlet of the desorber of approximately 15°C, and 10°C between the inlet and outlet of the resorber. This temperature jump has been taken as a valid case to continue with new simulation cases.

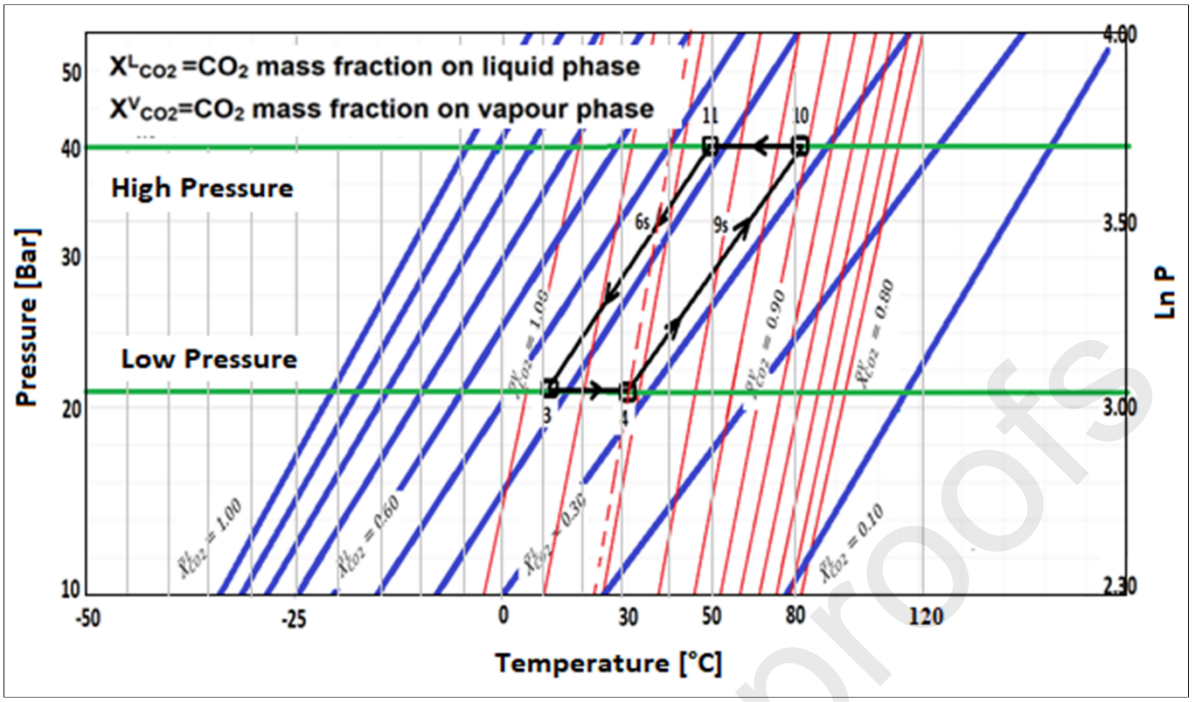

Figure 3. *Initial simulation case study of CO2/Acetone mixture*

Lastly, a combination of the operating intervals of the variables of the compression/resorption heat pump cycle using the CO_2/Acetone mixture allows the determination of the simulation of studies case for the parametric analysis of the cycle. In this sense, table 5 presents a summary of the study cases determined by varying the temperature of the solution at the desorber outlet from 30 to 70ºC with increments of 20ºC, ΔX between 0.10 and 0.20 with increments of 0.05, the temperature of the solution at the resorber outlet from 50 to 110ºC with increments of 10ºC, high pressure in the heat pump cycle between 30 and 50 bar with increments of 10 bar and a vapour mass flow value of 0.5 and 1 kg×s^{-1}, where:

- $T_{(4)}$: Desorber outlet temperature – solution side
- $T_{(11)}$: Resorber outlet temperature – solution side
- $\Delta X = X_{global} - X_l$: Composition difference between the global concentration of CO_2 in the mixture and poor solution
- P_{high}: Heat pump cycle high pressure
- $\dot{m}_v$: Vapour mass flow

Table 5. *Parameter for the simulation of the heat pump cycle compression/resorption using CO2/acetone mixture.*

P_{high} 30 Bar					
$T_{(4)}$ 30C°					
ΔX 10		***ΔX 15***		***ΔX 20***	
$T_{(11)}$ C°	**$\dot{m}_v$ kg×s^{-1}**	**$T_{(11)}$ C°**	**$\dot{m}_v$ kg×s^{-1}**	**$T_{(11)}$ C°**	**$\dot{m}_v$ kg×s^{-1}**

50	0.5	50	0.5	50	0.5
50	1	50	1	50	1
60	0.5	60	0.5	60	0.5
60	1	60	1	60	1
70	0.5	70	0.5	70	0.5
70	1	70	1	70	1
P_{high} 40 Bar					
$T_{(4)}$ 50C°					
ΔX 10		***ΔX 15***		***ΔX 20***	
$T_{(11)}$ C°	**$\dot{m}_v$ kg×s^{-1}**	**$T_{(11)}$ C°**	**$\dot{m}_v$ kg×s^{-1}**	**$T_{(11)}$ C°**	**$\dot{m}_v$ kg×s^{-1}**
70	0.5	70	0.5	70	0.5
70	1	70	1	70	1
80	0.5	80	0.5	80	0.5
80	1	80	1	80	1
90	0.5	90	0.5	90	0.5
90	1	90	1	90	1
P_{high} 50 Bar					
$T_{(4)}$ 70C°					

ΔX 10		*ΔX 15*		*ΔX 20*	
$T_{(11)}$ C°	$\dot{m}_v$ kg×s^{-1}	$T_{(11)}$ C°	$\dot{m}_v$ kg×s^{-1}	$T_{(11)}$ C°	$\dot{m}_v$ kg×s^{-1}
90	0.5	90	0.5	90	0.5
90	1	90	1	90	1
100	0.5	100	0.5	100	0.5
100	1	100	1	100	1
110	0.5	110	0.5	110	0.5
110	1	110	1	110	1

Table 5 shows that for each high-pressure value of the cycle (30, 40 and 50 bar), two study cases have been defined with respect to the vapour mass flow rate, of these three study cases are determined concerning the temperature of the solution at the outlet of the resorber as a boundary condition, the difference in composition between the global concentration of CO_2 in the mixture and lean solution and the temperature of the solution at the outlet of the desorber. In this way, regarding different temperatures on the desorber (30, 50 and 70°C) and the difference composition of CO_2 concentration (10, 15 and 20 ΔX) there are 18 possible combinations for each high pressure of the cycle (30, 40 and 50 bar), the total number of cases studied is 54. Furthermore, the energy efficiency of this equipment is characterized through the Operating Coefficient (COP) defined as the ratio of the heat produced Q_2 divided by the work consumed W. The energy balance in the heat pump allows us to relate the energy exchanges in form of heat and work that take place, $Q_1 + W = Q_2$, and the COP = Q_2/W [54].

3. Results and discussion

Following the methodology expressed by previous research that used the Peng-Robinson equations and correlated its findings, it was possible to determine a model of the properties and thermodynamic cycle of a thermal pump based on a mixture of CO_2 / Acetone. In this sense, the following sub-themes present the results obtained.

3.1. Parameters of binary interaction for the mixture CO_2/Acetone

Through the realization of the adjustment of the database available and the calculations with the Peng-Robinson equations for the mixture CO_2 / Acetone, the parameters of binary interaction for different

temperatures were obtained and are presented in table 6 and the results for the coefficients k_1, k_2 and k_3 found are presented in table 7.

Table 6. *K_{12} parameters for different temperatures*

Temperature (K)	K_{12}
291.15	-0.00516
298.15	0.01097
303.15	0.00794
313.15	-0.00630
333.15	-0.05077
353.15	-0.11221
373.15	-0.17869
393.15	-0.23040

Table 7. *k coefficients for binary interaction parameters*

Temperature (K)	k1	k2	k3
291.15 – 393.15	1.1139×10^{-4}	8.501×10^{-6}	-2.851×10^{-3}

The results obtained when using these coefficients in the calculation of compositions of the liquid and vapor phases, were compared with the experimental ones of Hsieh & Vrabec, [40], Chiu et al., [41] and Han et al., [39], obtaining a maximum mean square desviation of 4.28 %, 6.91 % and 8.70 %, respectively. The comparison of the data obtained through the use of these coefficients (Equation 20) in the present work with those obtained experimentally in the cited works, is shown in the graphs provided in appendix B.

Regarding the density of the mixture in the liquid phases, the results obtained with the model were compared with the experimental ones obtained by Ramírez-Ramos et al [42], obtaining a maximum square deviation of 13.4 %. The data fit for the density in the liquid phase of the mixture was improved using the Peneloux specific volume correction term [52]. In this case, the maximum square deviation values of 2.45 % and 4.11 % for the liquid phase and vapour, respectively. Regarding the deviation found between experimental data and those calculated for the excess enthalpy data of Ramírez-Ramos et al [42] a maximum deviation of 5.35 % was obtained.

3.2. Vapour Pressure diagram

The graphic of vapour pressure is also known as the diagram of VLE or bell, regarding the results obtained in different temperatures, figure 4 displays the pressure of the liquid-saturated vapour phases of the CO_2 / Acetone mixture as a function of the CO_2 composition from 0.10 in mole fraction to pure

CO_2 from 15ºC to 120ºC of temperature. Each point on the graph represents a case of vapor-liquid equilibrium for a given temperature, pressure, and CO_2 composition in the CO_2/acetone mixture.

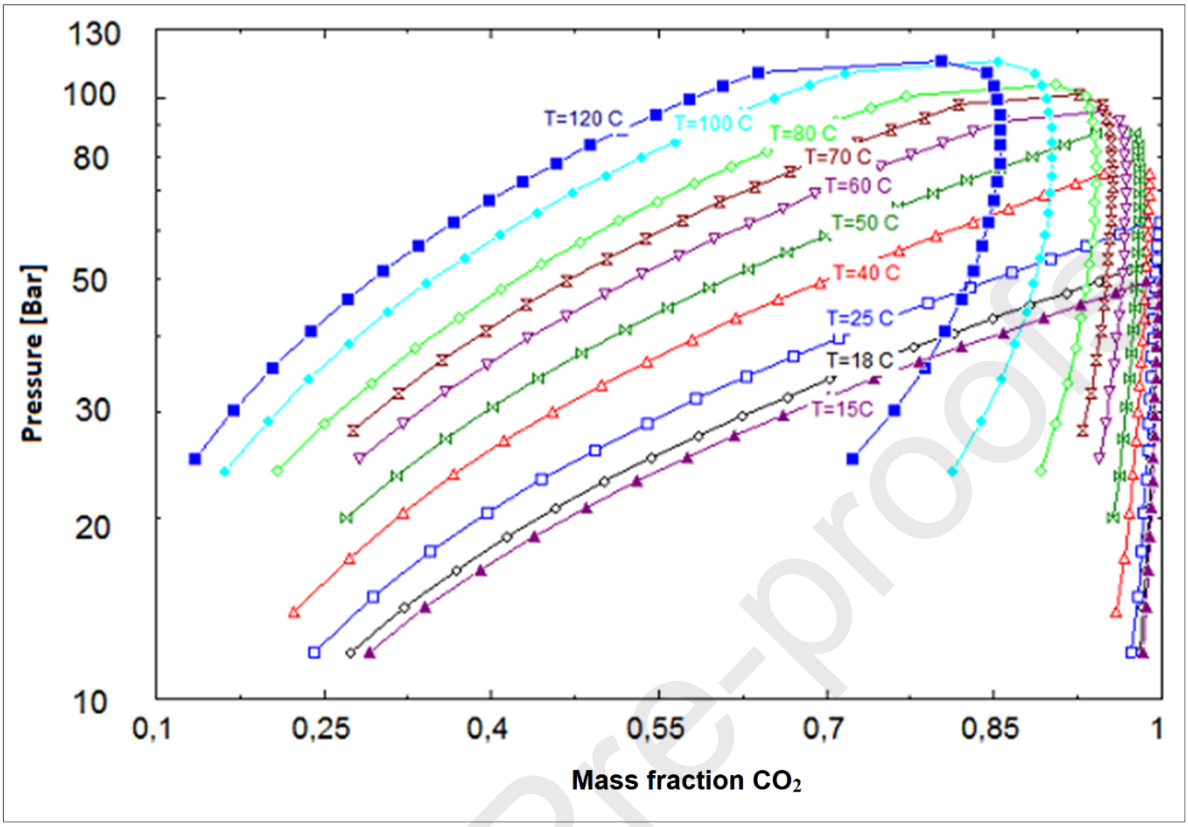

Figure 4. *Vapour Pressure of CO_2/Acetone mixtures against CO_2 mass fraction at different temperatures calculated with Peng-Robinson EoS*

It is shown that the pressure rises constantly as the molar composition of CO_2 in the mixture increases until it reaches the critical point at each temperature. From the critical point found there is a sudden drop in the composition corresponding to the saturated vapour phase, the increment of pressure with the increase of CO_2 is possible due to the critical pressure difference between the two compounds, meaning that a greater critical pressure allows to reach higher pressures until it drops. This behaviour has a similarity to the research performed by Bamberger & Maurer [55], who compared the CO_2/Acetone mixture from several research . The data obtained for the graph show that the minimum - maximum value of pressure and temperature at which the mixture is in liquid and saturated vapour are 12 - 120 bar and 15 - 120ºC, respectively. The minimum global composition of CO_2 to obtain saturated vapour is 0.75 at 120ºC, this concentration value rises to values close to 1 if the temperature decreases to a minimum of 15ºC. The top moves to the right to decrease the equilibrium temperature of the CO_2 / Acetone mixture. Fábián et al., [56] carried out an analysis of acetone dissolved in CO_2 in 11 different compositions in a range of temperatures from 50 to 100 K close to the critical point. Here it was found that the critical temperature of the mixture changes in direct relation to the composition, likewise the critical pressure reaches a maximum around the value of the acetone mole fraction of 0.3, and the critical density could also present a maximum molar fraction of 0.2 of acetone. In addition, this work validates the applicability of molecular modelling for the determination of the vapor-liquid equilibrium in CO_2/acetone mixtures. The equilibrium results of this work (Pressure, composition, and temperature) have been compared with those of the present research. In this way, the comparison denotes an average standard deviation of 10% has been obtained with respect to the pressure in a composition of 0.40 to 0.90 of CO_2 dissolved in Acetone in a temperature range between 298 and 393 K. This shows that the correlation obtained for the present work corresponds to other investigations that have studied the behaviour of the CO_2/Acetone mixture under different conditions of pressure, composition, and temperature.

On the other hand, based on the Clausius-Clapeyron equation, the Duhring diagram of the CO_2 / Acetone mixture is made, where figure 5 shows the graphical representation of the vapour pressure versus (-T) $*$ 1000;$T\ in\ K$, for different compositions of the liquid phase and saturated vapour. This diagram of Duhring is particularly useful when representing the thermodynamic cycle of the heat pump because it allows for visualizing the values of the pressures, temperatures and compositions of the cycle currents operating with the working mixture. In this way, knowing the operation conditions of CO_2, allows to determinate how the fluid will behave on the cycle regarding the need of separate one compound from other by vaporization.

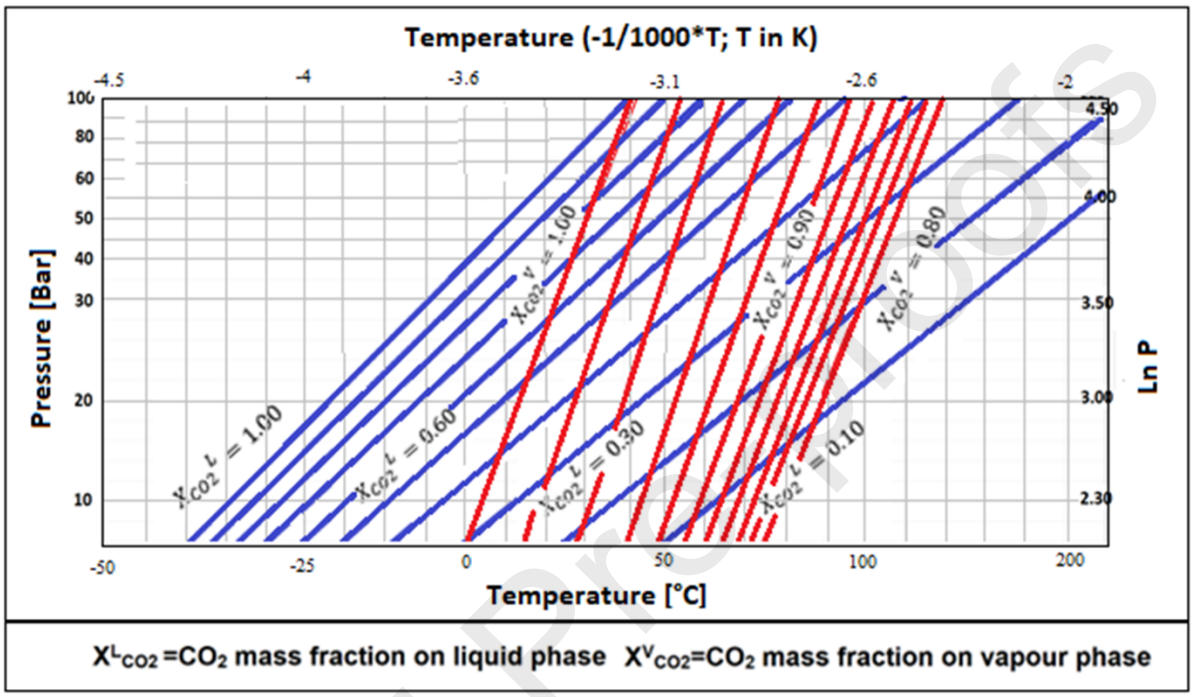

Figure 5. *Diagram PTXY (Duhring) of CO_2/Acetone mixture*

3.3. Density

The calculation of the density of the compound required the coefficients of the correlation of experimental data expressed in table 8. In this sense, the molar fraction of the CO_2 in the expression X_{CO_2} retrieves the following coefficients required in equation (26).

Table 8. *Coefficient of correlation*

Coefficient	Value
ρ_{00}	0.5439
ρ_{10}	0.08759
ρ_{01}	0.2207

ρ_{20}	0.02544
ρ_{11}	0.107
ρ_{02}	0.09804
ρ_{21}	0.03737
ρ_{12}	0.1037
ρ_{03}	0.08257

The results obtained with the Peng-Robinson equation of state regarding the density of the CO_2/Acetone mixture in the liquid and vapour phases were compared with the experimental data obtained by Ramírez-Ramos et al., [42]. In this sense, a maximum, medium and minimum deviation of 13.4, 5.2 and 2.4 %, respectively was obtained, and by using these three values, obtaining a better adjustment The data for the density in the liquid phase of the mixture was improved using the Péneloux volume correction term [52], being in this case the maximum, medium and minimum deviation values of 2.5, 1.8 and 0.8 % for the liquid and 4.1, 3.2 and 1.2 % for the vapour phase. Furthermore, figure 6 shows the comparison of the density data in the liquid phase of the CO_2/Acetone mixture obtained by Ramírez-Ramos et al., [42], with the model established in the present work. That comparison was made over a temperature range between 18 and 120 °C, a CO_2 mole fraction of 0.05 to 0.814, and pressure between 0.03 and 8.715 MPa.

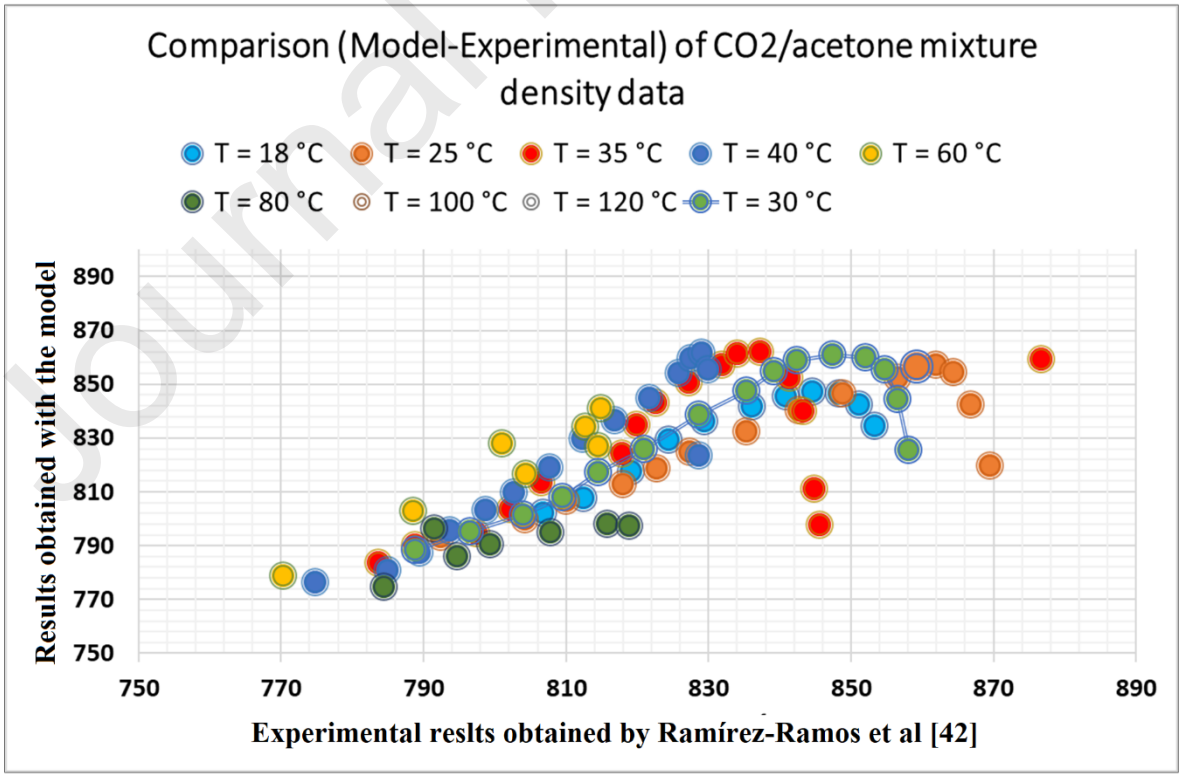

Figure 6. *Comparison (Model-Experimental) of CO2/acetone mixture density data*

On the other hand, the excess enthalpy values have been calculated with the Peng-Robinson equation of state and have been compared with the experimental data presented by Ramírez-Ramos et al., [42] in the defined range of pressure, temperature and molar composition of CO_2 in the CO_2/Acetone mixture. From this comparison, a maximum, medium and minimum deviation of 5.4, 3.5 and 1.3 %, respectively, have been obtained.

3.4. Parametric study

The equations described from 2.1 to 2.4 are taken from existing equations of state, however it has been determined that the Peng - Robinson equation of state is the most suitable due to a smaller deviation between experimental and simulation data by the approximation cited in 3.1 to 3.3

The parametric analysis of the compression/resorption heat pump cycle using the CO_2/Acetone mixture has been developed to analyse the influence of the independent variables of the cycle when one of them remains constant. This analysis makes it possible to determine the behaviour of the CO_2/Acetone mixture in this type of heat pump cycles. The mixture constitutes a new working fluid for this type of application, thus extending the use of this zeotropic mixture.

In this way, the results that are presented as follows comes from the software simulations which represent a presents clear tendency of a decreasing COP at higher temperatures. Regarding the validity of using computational simulations, the research of Cao et al. [57] on the utilization of zeotropic mixtures for an enhanced heat pump simulated with MATLAB has a response with the same tendency of COP vs condenser temperature, showing an important agreement with experimental results, meaning reliability on the simulated results. In this sense, the COP results of the compression/resorption heat pump cycle at a resorber outlet solution temperature between 50 and 70ºC, ΔX between 0.10 and 0.20, for an outlet solution temperature of the desorber (T_{des}) at 30°C, at a pressure of a) 30, b) 40 and c) 50 bar. The figure of this results can be found on appendix A under figure A1 and shows that if the high pressure of the cycle is constant and the temperature of the solution at the outlet of the resorber is 50ºC, the value of the operating coefficient reaches the higher conditions up to a maximum of 3. If P_{high} increases its value from 30 to 50 bar, the value of the heat pump cycle operation coefficient decreases to a minimum value of 1.01, a thermal jump of 20ºC and an increasing ΔX from 0.10 to 0.20 increases the value of COP. Furthermore, it was found that the value of the vapour mass flow rate ($\dot{m}_v$) does not influence the determination of the heat pump cycle operation coefficient, since the calculated COP values are superimposed on the graph.

On the other hand, the results of the heat pump cycle operation coefficient with a solution temperature at the desorber outlet of 50ºC, with a solution temperature at the resorber outlet between 70 and 90ºC, ΔX between 0.10 and 0.20 at a pressure of a) 30, b) 40 and c) 50 bar is displayed on figure A2 from appendix A. In this way, this figure shows that the COP values decrease to values close to 1 when the temperature of the solution at the outlet of the resorber increases from 70 to 90ºC. The highest value of COP in this case is 2.10, this is obtained with a value of ΔX of 0.20, a temperature of the solution at the outlet of the resorber of 70ºC at a pressure of 50 bar. If the cycle high pressure increases from 30 to 40 bar, the value of the heat pump cycle operation coefficient is reduced when ΔX =0.10. However, for ΔX =0.15 and 0.20, it is shown that for a value of P_{high} between 40 and 50 bar, the value of COP can be found from null to very close to 1 when there is a temperature jump between source and sink of 30ºC or higher. It has been determined that under these conditions the cycle does not operate as a compression/resorption heat pump when using the CO_2/acetone mixture as the working fluid.

Furthermore, figure A3 from appendix A shows the COP values determined when the temperature of the solution at the outlet of the desorber is 70ºC, a temperature of the solution at the outlet of the resorber between 90 and 110ºC, ΔX between 0.10 and 0.20, at a pressure of a) 30, b) 40 and c) 50 bar. In this

way, the results show that at a 30 bar heat pump cycle P_{high} the COP values have been determined only when ΔX is between 0.10 and 0.15, at ΔX of 0.20 the solution is in a state of saturation. The highest calculated COP value is 2, this is obtained with a high cycle pressure of 40 bar, a solution temperature at the resorber outlet of 90ºC and ΔX is 0.20. It has been determined that a temperature jump between the heat source and the sink of 20 ºC and 30ºC is feasible for the compression/resorption heat pump cycle, with a heat source temperature of 70ºC at a high cycle pressure of 40 bar, except for ΔX = 0.10. In this way, the results of the operation coefficient show a better performance of the compression/resorption heat pump cycle with a high pressure between 30 and 40 bar. A solution temperature at the desorber outlet of 30ºC improves the efficiency of the cycle, up to a maximum value of COP_{max}=3. If the largest thermal jump determined between the heat source and sink of the compression/resorption heat pump cycle using the CO_2/acetone mixture is 20ºC, the value of the cycle operation coefficient is increased until reaching the highest values, determined at each high pressure of the cycle. It has been determined that it is possible to generate heat pump cycle sink temperature by compression/resorption using the CO_2/acetone mixture of up to 100ºC with a source temperature of 70ºC, a difference between global composition and a lean composition (ΔX) of 0.20 and an P_{high} at 40 bar. In the same way, is important to mention the stability presented in the CO_2 concentration, compared to the research of Pan et al [28], that analysed the behaviour of the 4 zeotropic mixtures of CO_2 with the refrigerants R32, R134a, R152a and R290 on a regenerative supercritical CO_2 Bryton Cycle, that showed that the mass fraction of CO_2 provoke a decrement on the COP as it increased until reaching a lower state and then it starts to grow [28]. In this sense, the present system shows that for almost every condition, a greater CO_2 concentration means better performance, making it more reliable to predict its behaviour.

Moreover, a summary of the calculated values of the coefficient of operation (COP) as a function of the temperature of the solution at the desorber outlet (30, 50 and 70ºC), the temperature of the solution at the outlet of the resorber between (50 and 100ºC), a vapour mass flow rate ($\dot{m}_v$) of 0.5 and 1 $kg \times s^{-1}$, ΔX between 0.10 and 0.20, at a pressure of 30, 40 and 50 bar, are presented in the figure 5: a, b and c, respectively. In this way, figure 7.a shows that the coefficient of operation of the heat pump cycle (COP) decreases from 3 to 1.2 when the temperature of the solution at the desorber outlet increases from 30 to 50ºC. It is observed that the best performance of the cycle occurs when the difference in composition between the global concentration of CO_2 in the mixture and lean solution (ΔX) has a value between 0.15 and 0.20. The operating coefficient of the heat pump cycle decreases when the temperature of the solution at the outlet of the resorber increases from 50 to 100ºC. The effect of the vapour mass flow rate is not relevant since the COP values overlap for both cases (0.5 and 1 $kg \times s^{-1}$).

On the other hand, figure 7.b shows that if the high pressure of the cycle is 40 bar, the coefficient of operation of the heat pump cycle (COP) decreases when the temperature of the solution at the desorber outlet increases from 30 to 70ºC. The values of the coefficient of operation of the heat pump cycle increase to a maximum value of 2.8 with ΔX = 0.20. The COP of the cycle is reduced to a minimum value of 1.01 when the temperature of the solution at the outlet of the resorber increases from 50 to 70ºC, this happens at ΔX=0.10. It is shown that a thermal revaluation is feasible from a source temperature of 70ºC to a sink temperature of 100ºC. Furthermore, the research developed by Moreira Da-silva et al. [58] presented similar modelling of the compression/resorption cycle of the mixture CO_2/Acetone for air-conditioning in typical thermal conditions, where the temperature at the resorber outlet was 35°C and two cases were considered the first with ΔX=0.2 and the second with ΔX=0.3, regarding the same P_{high} = 40 in both cases, leading to a COP of 3.58 for case 1 and 2.71 for case 2 [58]. In this way, at ΔX=0.2 the COP of the two models is similar in that it was proven that a higher temperature at the desorber outlet means a lower COP, and even more, the difference between a poor and a rich mixture has an impact that is shown in the great COP of ΔX= 0.3.

Furthermore, figure 7.c shows that the heat pump cycle operating coefficient (COP) decreases when the temperature of the solution at the desorber outlet increases by 30 to 70ºC at a high pressure of 50 bar. A composition difference between the global concentration of CO_2 in the mixture and poor solution ΔX = 0.20 increases the values of the operating coefficient of the heat pump cycle (COP), up to a maximum of COP=2.6. If the temperature of the solution at the outlet of the resorber increases from 50 to 100ºC,

the COP of the cycle drops to a minimum value of 1.1. The maximum temperature of the solution at the outlet of the resorber for these conditions, where the cycle works as a heat pump, is 100ºC at a pressure of 40 bar.

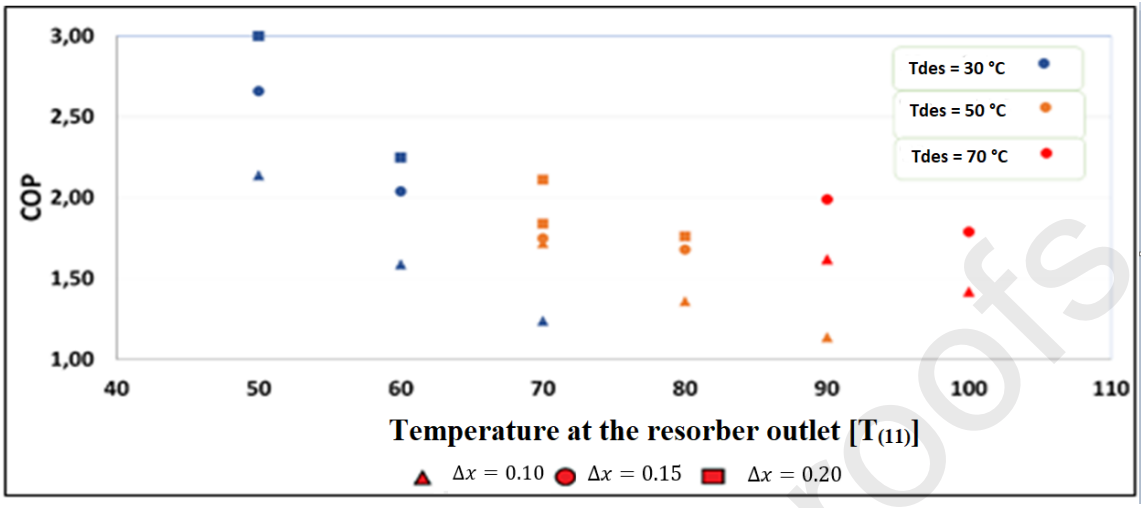

a)

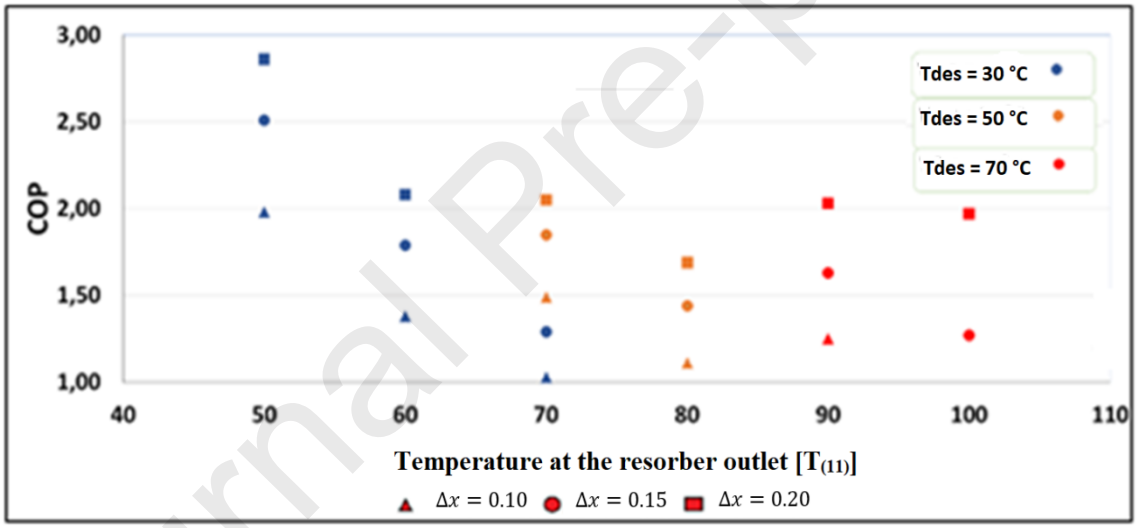

b)

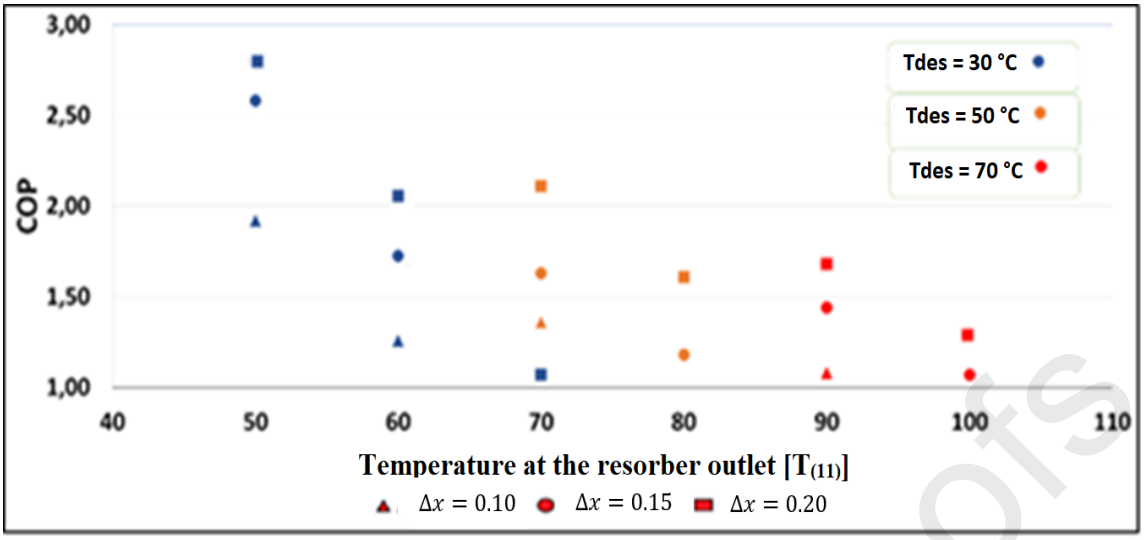

c)

Figure 7. *COP at a P_{high} at a) 30 bar b) 40 bar c) 50 bar*

Globally, if the temperature of the solution at the outlet of the desorber increases from 30 °C to 70 °C at the same pressure value, the performance of the compression/resorption heat pump cycle decreases from a maximum value from 3 to 1.1. The best global performance of the compression/resorption heat pump cycle occurs with a range of Δx (Composition difference between the global concentration of CO_2 in the mixture and poor solution) between 0.15 and 0.20. If the high cycle pressure increases, the cycle performance decreases. On the other hand, if the temperature of the solution at the outlet of the resorber increases along with the temperature at the outlet of the desorber, the performance of the cycle decreases. In this way, it is shown that the variation in the vapour mass flow from 0.5 to 1 kg×s^{-1} does not affect the operating coefficient of the cycle, since the results overlap with each other.

This phenomenon was also observed in the research of Gao et al. who reports that the elevated temperature results in an increment of the ratio pressure and discharge temperature of the system leading to a deterioration of the performance on the compression cycle [13]. In this sense, it is recommended that the solution temperature at the outlet of the desorber not exceed 40ºC and a break of this with the sink temperature of 20ºC. Furthermore, when comparing the utilization of transcritical CO_2 on water heating applications, it has been found by F. Cao et al. [59] on experiments with internal heat exchangers and conditions of ambient, water inlet and water outlet temperature of 16; 10 and 70°C respectably, that the COP reaches a value of 3.76 without heat exchanger and 3.81 with heat exchanger. In this way, experimentally, using trasncritical CO_2 bring a better COP than the best CO_2/Acetone mixture of 3.58. However, the presented zeotropic mixture allows to operate on subcritical conditions, allowing to reduce prices on equipment for lower pressures, granting at the same time acceptable COP values.

On the other hand, another important parameter that denotes the performance of the heat pump cycle is the ratio flow rate between the poor solution and the refrigerant expressed as ($f = \dot{m}_l / \dot{m}_v$). In this way, the ratio flow rate when the high pressure in the cycle is 30 bar has the highest calculated values (f = 7.1) with a composition difference between the global concentration of CO_2 in the mixture and poor solution (ΔX) of 0.10 is displayed in figure 8.a, showing that the solution temperature at the desorber outlet has a very slight influence on the ratio flow rate. The solution temperature at the resorber outlet is also not a variable that considerably influences the ratio flow rate. The values range in which the flow rate ratio is found for this pressure (30 bar) is between 3 and 7.1. The effect of the rate vapour mass flow is not relevant since the COP values overlap for both cases (0.5 and 1 kg×s^{-1}).

The highest ratio of solution value and rates vapour flow in the cycle for high pressure of 40 bars f = 6.8 as shown in figure 8.b, this is obtained in the same way as for a 30 bar P_{high} with ΔX = 0.10. The range of values in which the ratio flow rate is found for this pressure (40 bar) is between 3 to 6.8. Comparing this interval of "*f*" with that determined for a P_{high} in the 30 bar heat pump cycle, a reduction between its higher and lower limits is shown.

The ratio of solution and vapour flows of the cycle at a pressure of 50 bar reaches a value f = 6.2 in figure 8.c, this is also determined with ΔX = 0.10, as in the cases with P_{high} of 30 and 40 bar. The range of values in which the ratio flow rate is found for this pressure (40 bar) is between 2.5 to 6.2. On the other hand, the temperature of the solution at the outlet of the desorber, the temperature of the solution at the outlet of the resorber and the rate mass flow of vapour do not strongly influence the ratio flow rate *f*.

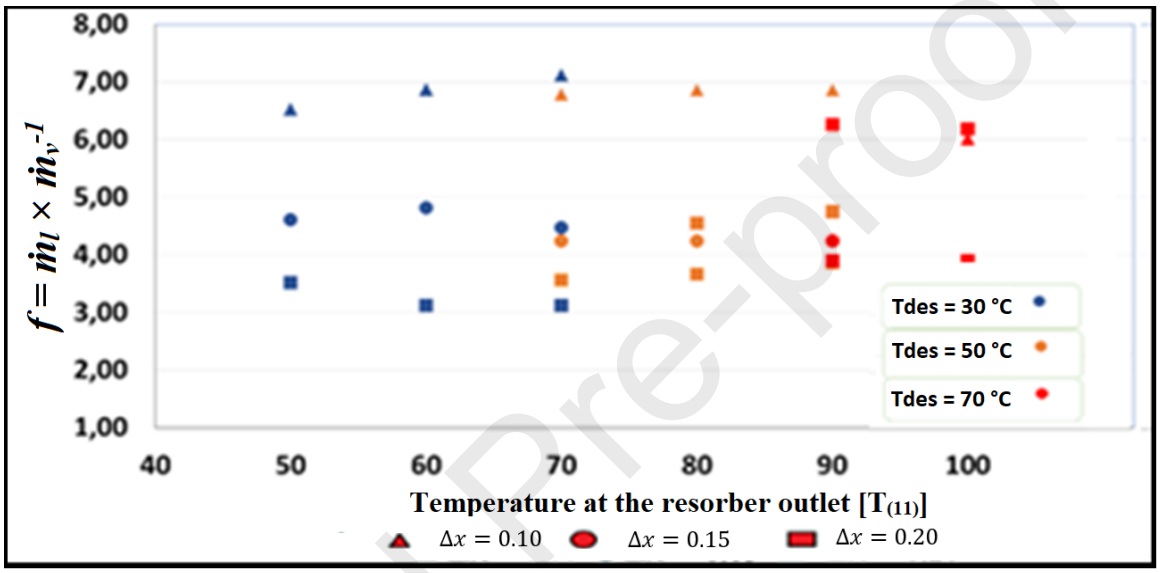

a)

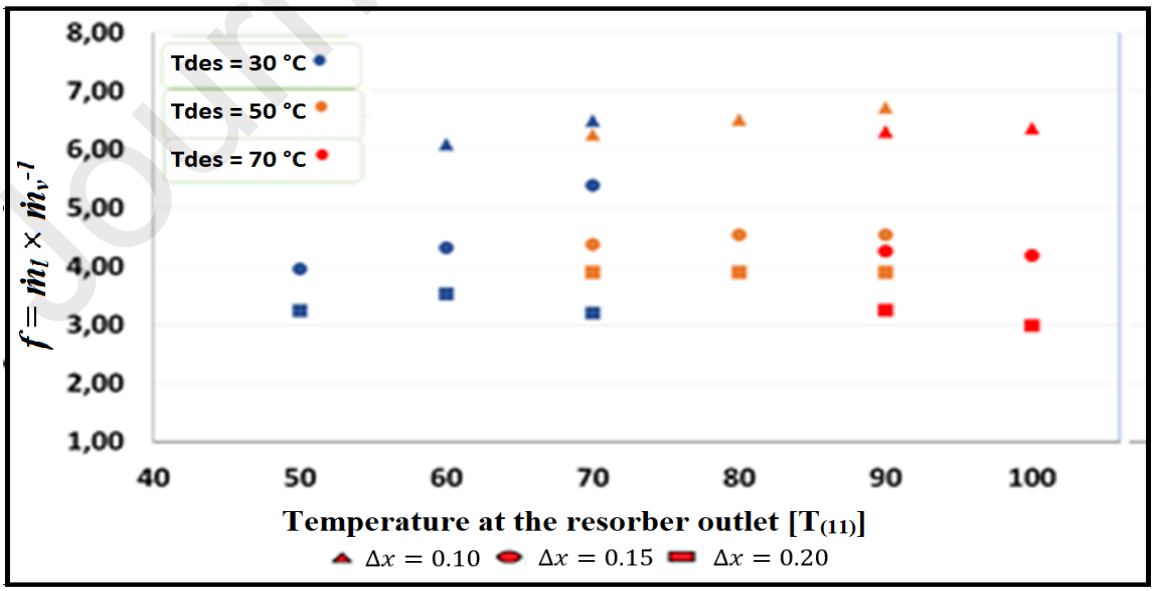

b)

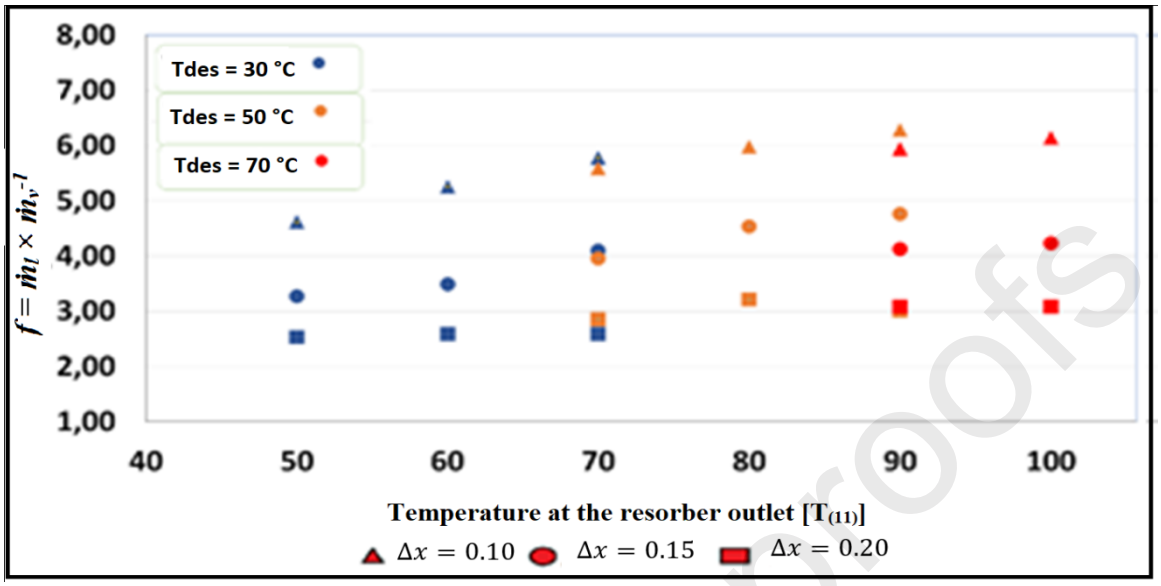

c)

Figure 8. *Flow rate ratio (f) at a high cycle pressure of a)30 bar b) 40 bar c) 50 bar*

In general, the values calculated for the ratio flow rate are in the range between 2.5 and 7.1 minimum and maximum, respectively. The highest calculated values for the ratio flow rate *f* occur when ΔX is 0.10. The increase in high pressure in the cycle represents a decrease in the flow rate ratio. The variation in the rate vapour mass flow from 0.5 to 1 kg×s $^{-1}$does not affect the calculated ratio flow rate since the results overlap with each other. However, it's important to mention that regarding the increment on rate pressure flow also become lower, in this sense, the research of Jensen et al. [27], on the development of absorption-compression heat pumps based on ammonia-water mixtures, concluded that for circulating ratios lower than 0.5 and rich concentrations of ammonia between 0.2 and 0.8 resulted on a considerable increment on the ratio pressure, which at the same time produced a reduction on the COP, making this kind of design not recommendable [27]. In this way, is important to consider the pressure proportions, mass friction and its results in flow ratio to maximize the enhancement of the COP on the system.

3.5 Comparison of results of the compression/resorption heat pump cycle using the CO2/acetone mixtures with related investigations

In a comparative way, a literature review was performed with related works on heat pumps that use CO_2 as a pure refrigerant (transcritical cycle) as well as combined with absorbents, to show a comparison of the data results obtained in the simulation of the compression/resorption heat pump cycle using the CO_2/Acetone mixture, which is displayed on table 9.

Table 9. Comparison of results of the compression/resorption heat pump cycle using the CO_2/acetone mixtures with related investigations

Reference	Description of work / product	Fluid	Fluid and Temp. at heat source (˚C)	Fluid and temperature achieved (˚C)	Power (kW)	COP
Present work [-]	Modelling of the compression/resorption heat pump cycle using the CO_2/Acetone mixture.	CO_2/ Acetone	Wastewater 30 - 70	Water 50 - 100	100 - 250	1.1 - 3
Mayekawa [60]	CO_2 transcritical heat pumps. Eco Sirocco	CO_2 transc. (R744)	Waste water 20 - 25	Air 100-120	65 - 90	2.9
Durr Therme CO2 [61]	Heat pump Thermeco2 HHR1000	CO_2 transc. (R744)	Waste water 8 - 40	Water 80- 110	51 - 2.2 MW	3.9
Oue T. and Okada K [62]	Semi-hermetic twin-screw inverter for industrial applications	R134a and R245fa Mixture	Air 10 - 40	Water 90	70 - 230	1.7 - 3

Continue Table 9. Comparison of results of the compression/resorption heat pump cycle using the CO_2/acetone mixtures with related investigations

Ochsner K [63]	Heat pump, model: IWWDSS R2R3b	R134a and OK01 Mixture	Waste water 35 - 55	Water 95 a 130	170 - 750	5.3

Okuda S et al [64]	Compact hot water heat pump with closed economizer and a two-stage turbocharger with intermediate injection. Model: ETW- L	R134 a	Waste water 10 - 50	Water 90	340 - 600	4.1

Considering the operating temperature range of the present work, it is shown to be one of the widest (30 to 70 °C) with reference to the temperature in the heat source compared to the other studies. Regarding the temperature in the sink, it is shown that the range determined between 50 and 100 °C for this work has a range quite similar to that of the Durr Thermea CO2 company [61], Kobe Steel - Kobelco [62] and Mitsubishi [64], considering that in all three works, the fluid to be heated is water. The range of calorific power calculated for the present work (100 to 250 kW) is very close to that presented in the work of the company Kobe Steel - Kobelco [62], which indicates that this technology is viable for its implementation using the CO_2/acetone mixture. Finally, the results obtained for the performance of the cycle show that the compression/resorption heat pump cycle using the CO_2/acetone mixture as working fluid is viable. The COP range calculated for this work is 1.1 to 3, this depends, as has been seen, on the conditions of temperature, pressure and molar composition of CO_2 in the CO_2/acetone mixture, where the cycle of the heat pump is operated. Furthermore, it can be considered that this range of COP is an average value for the ranges calculated by the works developed in the companies Mayekawa [60] of 2.9, Durr Thermea CO_2 [61] of 3.9, Kobe Steel - Kobelco [62] between 1.7 to 3 , and Mitsubishi [64] of 4.1. The highest efficiency recorded for a water heat pump cycle is the one presented by the company Ochsner Energie Tecnik GmbH [63] when using the R134a Mix + OK01 mix as working pair, the COP reaches a value of 5.3.

4. Conclusions

The modelling of the utilization of a novel mixture of CO_2/acetone as a working fluid for compression/resorption heat pump is a technology that allows to move to non-hazardous and eco-friendly alternatives. In this research it was modelled this application on operative conditions of low heat waste exploitation showing promising results such as congruence with the literature and coefficient of performance increment under certain parameters.

The Peng Robinson equation of state was selected as the method to determine the equilibrium and other thermodynamic properties of the mixture. In this sense, it was used following the methodology of several authors, proving to be useful and the results validate its use for the CO_2/acetone mixture. In this way, the adjustment of equilibrium parameters of the CO_2/acetone mixture between experimental data obtained in the literature and calculated showed a maximum average square deviation of 4.28 % and 8.70 % for a temperature range between 291 to 303 K and 333 to 393 K, respectively. Even more, the calculation of the polynomial equation for the binary interaction parameter (k_{12}) in the model based on the cubic Peng Robinson equation of state showed that the most influential parameter for the fit is k_1.

On the other hand, the independent variables of the compression/resorption heat pump cycle and its operating range were determined by the range of experimental data found in the literature and the range was determined by the vapour pressure diagram of the mixture. In this way, the modelling of the heat pump cycle was based on the adjustment of matter and energy of each component of the cycle and a

hypothetical assumption of the state of the mixture at different points of the cycle in a simulated study case.

The analysis of the compression/resorption heat pump cycle using the CO_2/acetone mixture defines a range of CO_2 concentrations of 20 to 50 %. In this sense, a higher molar concentration of CO_2 improves the efficiency of the compression/resorption heat pump cycle, reaching heating temperatures in the sink up to 110 ºC. Furthermore, if the temperature of the solution at the desorber outlet increases from 30 ºC to 70 ºC, the cycle efficiency (COP) decreases from a value of 3 to 1.1. Even more, it was defined that the increase in high pressure (30 to 50 bar) is a determining parameter in cycle performance (COP).

On the other hand, the highest value of the operation coefficient of the compression/resorption heat pump cycle (COP=3) was determined when the composition difference between the global concentration of CO_2 in the mixture and poor solution (ΔX) is 0.20, the temperature of the solution at the outlet of the desorber is 30 ºC and the difference in temperature between source and sink is 20 ºC.

An important point to mention is that the COP value obtained in the cycle simulation was not affected by the variation of the steam mass flow rate.

Lastly, the flow rate ratio in the compression/resorption heat pump cycle showed to increase in value if the solution temperature at the desorber and resorber outlets increases from 30 to 70 °C and 50 to 110 °C, respectively. In this way, the highest value calculated in the flow rate ratio was 7.1, this value was determined at a molar concentration difference of CO_2 between the mixture line and the solution line (ΔX) of 0.10. The variable with the greatest influence on the flow rate ratio is the difference in molar concentration of CO_2 in the CO_2/Acetone mixture between the mixing line and the solution line.

On the other hand, the present modelling investigation reflected the parametric simulation to the construction and experimentation of an application model that has been developed on a continuous research. In this way, the following research will carry out an experimental study of the desorption process of the studied CO_2-Acetone mixture, considering the effects of a plate heat exchanger, Furthermore, considerations such as the geometry and operational limitations of the heat exchanger as a desorber will be analysed, to design, build and develop the experimental methodology to obtain results of the main parameters of heat and mass transfer, heat transfer coefficient of the solution, average vapour quality, desorption mass flow and heat flow in the exchanger. The experimental validation results obtained for the desorber will be defined on a working range (pressure, temperature and composition) and the operating conditions of the heat exchanger. The future study based on the present work will provide a scientific basis for the use of the CO_2/acetone mixture in compression/resorption heat pump cycles.

Acknowledgements

This study is part of an R&D project funded by the Ministry of Economy, Industry and Competitiveness of Spain (DPI2015-71306-R). Paúl Dávila thanks the Rovira i Virgili University for awarding the Martí-Franqués 2016 (2016PMF-PIPF-26) to obtain a PhD.

5. References

[1] J. Zhang, H. H. Zhang, Y. L. He, and W. Q. Tao, “A comprehensive review on advances and

applications of industrial heat pumps based on the practices in China," *Appl. Energy*, vol. 178, pp. 800–825, Sep. 2016, doi: 10.1016/J.APENERGY.2016.06.049.

[2] L. Jiang, R. Q. Wang, X. Tao, and A. P. Roskilly, "A hybrid resorption-compression heat transformer for energy storage and upgrade with a large temperature lift," *Appl. Energy*, vol. 280, p. 115910, Dec. 2020, doi: 10.1016/J.APENERGY.2020.115910.

[3] M. Wang, C. Deng, Y. Wang, and X. Feng, "Exergoeconomic performance comparison, selection and integration of industrial heat pumps for low grade waste heat recovery," *Energy Convers. Manag.*, vol. 207, p. 112532, Mar. 2020, doi: 10.1016/J.ENCONMAN.2020.112532.

[4] J. Jiang, B. Hu, R. Z. Wang, N. Deng, F. Cao, and C. C. Wang, "A review and perspective on industry high-temperature heat pumps," *Renew. Sustain. Energy Rev.*, vol. 161, p. 112106, Jun. 2022, doi: 10.1016/J.RSER.2022.112106.

[5] L. J. Goh, M. Y. Othman, S. Mat, H. Ruslan, and K. Sopian, "Review of heat pump systems for drying application," *Renew. Sustain. Energy Rev.*, vol. 15, no. 9, pp. 4788–4796, Dec. 2011, doi: 10.1016/J.RSER.2011.07.072.

[6] Z. Liu, S. Sun, H. Guo, and M. Gong, "Experimental study on the concentration shift characteristics in a single-stage recuperative heat pump with large temperature lift," *Appl. Therm. Eng.*, vol. 210, p. 118358, Jun. 2022, doi: 10.1016/J.APPLTHERMALENG.2022.118358.

[7] X. She, Y. Yin, and X. Zhang, "A proposed subcooling method for vapor compression refrigeration cycle based on expansion power recovery," *Int. J. Refrig.*, vol. 43, pp. 50–61, Jul. 2014, doi: 10.1016/J.IJREFRIG.2014.03.008.

[8] W. Wu, T. You, J. Wang, B. Wang, W. Shi, and X. Li, "A novel internally hybrid absorption-compression heat pump for performance improvement," *Energy Convers. Manag.*, vol. 168, pp. 237–251, Jul. 2018, doi: 10.1016/J.ENCONMAN.2018.05.007.

[9] P. Bouteiller, M.-F. Terrier, and P. Tobaly, "Experimental study of heat pump thermodynamic cycles using CO2 based mixtures - Methodology and first results," *AIP Conf. Proc.*, vol. 1814, no. 1, p. 20052, Feb. 2017, doi: 10.1063/1.4976271.

[10] Y. Cao, H. A. Dhahad, A. M. Mohamed, and A. E. Anqi, "Thermo-economic investigation and multi-objective optimization of a novel enhanced heat pump system with zeotropic mixture using NSGA-II," *Appl. Therm. Eng.*, vol. 194, p. 116374, Jul. 2021, doi: 10.1016/J.APPLTHERMALENG.2020.116374.

[11] K. J. Chua, S. K. Chou, and W. M. Yang, "Advances in heat pump systems: A review," *Appl. Energy*, vol. 87, no. 12, pp. 3611–3624, Dec. 2010, doi: 10.1016/J.APENERGY.2010.06.014.

[12] C. Arpagaus, F. Bless, M. Uhlmann, J. Schiffmann, and S. S. Bertsch, "High temperature heat pumps: Market overview, state of the art, research status, refrigerants, and application potentials," *Energy*, vol. 152, pp. 985–1010, Jun. 2018, doi: 10.1016/J.ENERGY.2018.03.166.

[13] J. T. Gao, Z. Y. Xu, and R. Z. Wang, "An air-source hybrid absorption-compression heat pump with large temperature lift," *Appl. Energy*, vol. 291, p. 116810, Jun. 2021, doi: 10.1016/J.APENERGY.2021.116810.

[14] Z. Xu and R. Wang, "Absorption heat pump for waste heat reuse: current states and future development," *Front. Energy*, vol. 11, no. 4, pp. 414–436, 2017, doi: 10.1007/s11708-017-0507-1.

[15] L. L. Vasiliev, D. A. Mishkinis, A. A. Antukh, A. G. Kulakov, and L. L. Vasiliev, "Resorption heat pump," *Appl. Therm. Eng.*, vol. 24, no. 13, pp. 1893–1903, Sep. 2004, doi: 10.1016/J.APPLTHERMALENG.2003.12.018.

[16] V. Gudjonsdottir, C. A. Infante Ferreira, G. Rexwinkel, and A. A. Kiss, "Enhanced performance of wet compression-resorption heat pumps by using NH3-CO2-H2O as working fluid," *Energy*, vol. 124, pp. 531–542, Apr. 2017, doi: 10.1016/J.ENERGY.2017.02.051.

[17] C. W. Jung, S. S. An, and Y. T. Kang, "Thermal performance estimation of ammonia-water plate bubble absorbers for compression/absorption hybrid heat pump application," *Energy*, vol. 75, pp. 371–378, Oct. 2014, doi: 10.1016/J.ENERGY.2014.07.086.

[18] H. Rostamzadeh, A. S. Namin, H. Ghaebi, and M. Amidpour, "Performance assessment and optimization of a humidification dehumidification (HDH) system driven by absorption-compression heat pump cycle," *Desalination*, vol. 447, pp. 84–101, Dec. 2018, doi: 10.1016/J.DESAL.2018.08.015.

[19] B. Markmann *et al.*, "Experimental results of an absorption-compression heat pump using the working fluid ammonia/water for heat recovery in industrial processes," *Int. J. Refrig.*, vol. 99, pp. 59–68, Mar. 2019, doi: 10.1016/J.IJREFRIG.2018.10.010.

[20] T. Jia, E. Dai, and Y. Dai, "Thermodynamic analysis and optimization of a balanced-type single-stage NH3-H2O absorption-resorption heat pump cycle for residential heating application," *Energy*, vol. 171, pp. 120–134, Mar. 2019, doi: 10.1016/J.ENERGY.2019.01.002.

[21] M. U. Ahrens *et al.*, "Identification of Existing Challenges and Future Trends for the Utilization of Ammonia-Water Absorption–Compression Heat Pumps at High Temperature Operation," *Appl. Sci.*, vol. 11, no. 10, 2021, doi: 10.3390/app11104635.

[22] A. A. Roeder, A. Goyal, and S. Garimella, "Transient simulation of ammonia–water mixture desorption for absorption heat pumps," *Int. J. Refrig.*, vol. 100, pp. 354–367, Apr. 2019, doi: 10.1016/J.IJREFRIG.2019.01.032.

[23] L. G. Farshi and S. Khalili, "Thermoeconomic analysis of a new ejector boosted hybrid heat pump (EBHP) and comparison with three conventional types of heat pumps," *Energy*, vol. 170, pp. 619–635, Mar. 2019, doi: 10.1016/J.ENERGY.2018.12.155.

[24] V. Gudjonsdottir and C. A. Infante Ferreira, "Technical and economic analysis of wet compression–resorption heat pumps," *Int. J. Refrig.*, vol. 117, pp. 140–149, Sep. 2020, doi: 10.1016/J.IJREFRIG.2020.05.010.

[25] T. Jia, P. Dou, P. Chu, and Y. Dai, "Proposal and performance analysis of a novel solar-assisted resorption-subcooled compression hybrid heat pump system for space heating in cold climate condition," *Renew. Energy*, vol. 150, pp. 1136–1150, May 2020, doi: 10.1016/J.RENENE.2019.10.062.

[26] W. Wongsuwan, S. Kumar, P. Neveu, and F. Meunier, "A review of chemical heat pump technology and applications," *Appl. Therm. Eng.*, vol. 21, no. 15, pp. 1489–1519, Oct. 2001, doi: 10.1016/S1359-4311(01)00022-9.

[27] J. K. Jensen, W. B. Markussen, L. Reinholdt, and B. Elmegaard, "On the development of high temperature ammonia–water hybrid absorption–compression heat pumps," *Int. J. Refrig.*, vol. 58, pp. 79–89, Oct. 2015, doi: 10.1016/J.IJREFRIG.2015.06.006.

[28] M. Pan, X. Bian, Y. Zhu, Y. Liang, F. Lu, and G. Xiao, "Thermodynamic analysis of a combined supercritical CO2 and ejector expansion refrigeration cycle for engine waste heat recovery," *Energy Convers. Manag.*, vol. 224, p. 113373, Nov. 2020, doi: 10.1016/J.ENCONMAN.2020.113373.

[29] B. Zühlsdorf, J. K. Jensen, S. Cignitti, C. Madsen, and B. Elmegaard, "Analysis of temperature glide matching of heat pumps with zeotropic working fluid mixtures for different temperature glides," *Energy*, vol. 153, pp. 650–660, Jun. 2018, doi: 10.1016/J.ENERGY.2018.04.048.

[30] Y. Zhao, B. Yu, B. Wang, S. Zhang, and Y. Xiao, "Heat integration and optimization of direct-fired supercritical CO2 power cycle coupled to coal gasification process," *Appl. Therm. Eng.*, vol. 130, pp. 1022–1032, Feb. 2018, doi: 10.1016/J.APPLTHERMALENG.2017.11.069.

[31] G. Mozurkewich, L. D. Simoni, M. A. Stadtherr, and W. F. Schneider, "Performance implications of chemical absorption for the carbon-dioxide-cofluid refrigeration cycle," *Int. J. Refrig.*, vol. 46, pp. 196–206, Oct. 2014, doi: 10.1016/J.IJREFRIG.2014.06.014.

[32] Z. Jin, T. M. Eikevik, P. Nekså, A. Hafner, and R. Wang, "Annual energy performance of R744 and R410A heat pumping systems," *Appl. Therm. Eng.*, vol. 117, pp. 568–576, May 2017, doi: 10.1016/J.APPLTHERMALENG.2017.02.072.

[33] E. Groll and H. Kruse, "Kompressionskältemaschine mit lösungskreislauf für umweltverträgliche kältemittel," *KK Die Kälte und Klimatechnik*, vol. 45, pp. 206–218, 1992.

[34] G. Mozurkewich, M. L. Greenfield, W. F. Schneider, D. C. Zietlow, and J. J. Meyer, "Simulated performance and cofluid dependence of a CO2-cofluid refrigeration cycle with wet compression," *Int. J. Refrig.*, vol. 25, no. 8, pp. 1123–1136, Dec. 2002, doi: 10.1016/S0140-7007(02)00004-X.

[35] J. Wu, Q. Pan, and G. L. Rempel, "Pressure−Density−Temperature Behavior of CO2/Acetone, CO2/Toluene, and CO2/Monochlorobenzene Mixtures in the Near-Critical Region," *J. Chem. Eng. Data*, vol. 49, no. 4, pp. 976–979, Jul. 2004, doi: 10.1021/je0342771.

[36] A. Cavallini and C. Zilio, "Carbon dioxide as a natural refrigerant," *Int. J. Low-Carbon Technol.*, vol. 2, no. 3, pp. 225–249, Jul. 2007, doi: 10.1093/ijlct/2.3.225.

[37] J. A. Young, "Acetone," *J. Chem. Educ.*, vol. 78, no. 9, p. 1175, Sep. 2001, doi: 10.1021/ed078p1175.

[38] M. Stievano and N. Elvassore, "High-pressure density and vapor–liquid equilibrium for the binary systems carbon dioxide–ethanol, carbon dioxide–acetone and carbon dioxide–dichloromethane," *J. Supercrit. Fluids*, vol. 33, no. 1, pp. 7–14, Jan. 2005, doi: 10.1016/J.SUPFLU.2004.04.003.

[39] F. Han, Y. Xue, Y. Tian, X. Zhao, and L. Chen, "Vapor−Liquid Equilibria of the Carbon Dioxide + Acetone System at Pressures from (2.36 to 11.77) MPa and Temperatures from (333.15 to 393.15) K," *J. Chem. Eng. Data*, vol. 50, no. 1, pp. 36–39, Jan. 2005, doi: 10.1021/je049887v.

[40] C. M. Hsieh and J. Vrabec, "Vapor–liquid equilibrium measurements of the binary mixtures CO2 + acetone and CO2 + pentanones," *J. Supercrit. Fluids*, vol. 100, pp. 160–166, May 2015, doi: 10.1016/J.SUPFLU.2015.02.003.

[41] H.-Y. Chiu, M.-J. Lee, and H. Lin, "Vapor−Liquid Phase Boundaries of Binary Mixtures of Carbon Dioxide with Ethanol and Acetone," *J. Chem. Eng. Data*, vol. 53, no. 10, pp. 2393–

2402, Oct. 2008, doi: 10.1021/je800371a.

[42] G. E. Ramírez-Ramos, Y. Zgar, D. Salavera, Y. Coulier, K. Ballerat-Busserolles, and A. Coronas, "Vapor-liquid equilibrium, liquid density and excess enthalpy of the carbon dioxide+acetone mixture: Experimental measurements and correlations," *Fluid Phase Equilib.*, vol. 532, p. 112915, Mar. 2021, doi: 10.1016/J.FLUID.2020.112915.

[43] C. Liu, Z. Wang, W. Han, Q. Kang, and M. Liu, "Working domains of a hybrid absorption-compression heat pump for industrial applications," *Energy Convers. Manag.*, vol. 195, pp. 226–235, Sep. 2019, doi: 10.1016/J.ENCONMAN.2019.05.013.

[44] J. K. Jensen, T. Ommen, W. B. Markussen, L. Reinholdt, and B. Elmegaard, "Technical and economic working domains of industrial heat pumps: Part 2 – Ammonia-water hybrid absorption-compression heat pumps," *Int. J. Refrig.*, vol. 55, pp. 183–200, Jul. 2015, doi: 10.1016/J.IJREFRIG.2015.02.011.

[45] C. Liu, Y. Jiang, W. Han, and Q. Kang, "A high-temperature hybrid absorption-compression heat pump for waste heat recovery," *Energy Convers. Manag.*, vol. 172, pp. 391–401, Sep. 2018, doi: 10.1016/J.ENCONMAN.2018.07.027.

[46] Aspen Technology Inc, *Aspen Physical Property System*, V8.4. Burlington, USA: NIST Standard Reference Database 103b, 2013.

[47] D.-Y. Peng and D. B. Robinson, "A New Two-Constant Equation of State," *Ind. Eng. Chem. Fundam.*, vol. 15, no. 1, pp. 59–64, Feb. 1976, doi: 10.1021/i160057a011.

[48] A. Rivera-Alvarez, O. I. Abakporo, J. D. Osorio, R. Hovsapian, and J. C. Ordonez, "Predicting the Slope of the Temperature–Entropy Vapor Saturation Curve for Working Fluid Selection Based on Lee–Kesler Modeling," *Ind. Eng. Chem. Res.*, vol. 59, no. 2, pp. 956–969, Jan. 2020, doi: 10.1021/acs.iecr.9b05736.

[49] D. Siderus, "NIST Standard Reference Simulation Website - SRD 173," *National Institute of Standards and Technology*, 2017. https://data.nist.gov/od/id/FF429BC178798B3EE0431A570681E858232 (accessed Apr. 29, 2022).

[50] S. Klein and G. Nellis, *Thermodynamics*, 1st ed. Madison: Cambridge University Press, 2011.

[51] J. Rodríguez, "Estimación de propiedades termodinámica," in *Modelado, Simulación y Optimización de Procesos Químicos*, Buenos Aires: Universidad Tecnológica Nacional, 2000, pp. 303–343.

[52] A. Péneloux, E. Rauzy, and R. Fréze, "A consistent correction for Redlich-Kwong-Soave volumes," *Fluid Phase Equilib.*, vol. 8, no. 1, pp. 7–23, Jan. 1982, doi: 10.1016/0378-3812(82)80002-2.

[53] F. A. Aly and L. L. Lee, "Self-consistent equations for calculating the ideal gas heat capacity, enthalpy, and entropy," *Fluid Phase Equilib.*, vol. 6, no. 3–4, pp. 169–179, Jan. 1981, doi: 10.1016/0378-3812(81)85002-9.

[54] X. Song *et al.*, "Experimental study on heating performance of a CO2 heat pump system for an electric bus," *Appl. Therm. Eng.*, vol. 190, p. 116789, May 2021, doi: 10.1016/J.APPLTHERMALENG.2021.116789.

[55] A. Bamberger and G. Maurer, "High-pressure (vapour + liquid) equilibria in (carbon dioxide +

acetone or 2-propanol) at temperatures from 293 K to 333 K," *J. Chem. Thermodyn.*, vol. 32, no. 5, pp. 685–700, May 2000, doi: 10.1006/JCHT.1999.0641.

[56] B. Fábián, G. Horvai, A. Idrissi, and P. Jedlovszky, "Vapour-liquid equilibrium of acetone-CO2 mixtures of different compositions at the vicinity of the critical point," *J. CO2 Util.*, vol. 34, pp. 465–471, Dec. 2019, doi: 10.1016/j.jcou.2019.07.001.

[57] J. Cao, X. Feng, X. Ji, and X. Lu, "Study on the theoretical limit performance of multi-pressure evaporation ORC based on zeotropic mixture," *Huagong Xuebao/CIESC J.*, vol. 72, no. 7, pp. 3780–3787, 2021, doi: 10.11949/0438-1157.20210380.

[58] R. J. B. Moreira-da-Silva, D. Salavera, and A. Coronas, "Modelling of CO2/acetone fluid mixture thermodynamic properties for compression/resorption refrigeration systems," *{IOP} Conf. Ser. Mater. Sci. Eng.*, vol. 595, no. 1, p. 12030, Sep. 2019, doi: 10.1088/1757-899x/595/1/012030.

[59] F. Cao, Z. Ye, and Y. Wang, "Experimental investigation on the influence of internal heat exchanger in a transcritical CO2 heat pump water heater," *Appl. Therm. Eng.*, vol. 168, p. 114855, Mar. 2020, doi: 10.1016/J.APPLTHERMALENG.2019.114855.

[60] Mayekawa, "CO2 supercritical heat pump, HEAT CO2," 2016. .

[61] Thermea Durr, "CO2-Kaltemaschinen und Hochtemperaturw armepumpen," 2017.

[62] T. Oue and K. Okada, "Air-sourced 90°C hot water supplying heat pump, 'hEM-90A,'" *R D Res. Dev. Kobe Steel Eng. Reports*, vol. 63, no. 2, pp. 47–50, 2013.

[63] K. Ochsner, "High temperature heat pumps for waste heat recovery," in *European heat pump Association (ehpa)*, 2018, p. 44.

[64] S. Okuda, K. Ueda, S. Shibutani, Y. Shirakata, N. Matsukura, and Y. Togano, "Heat Application Technology by Centrifugal Heat Pump ETW Series for Hot Water - Continuous Supply of Hot Water at temperature of 90°C," 2011.

6. Appendix A

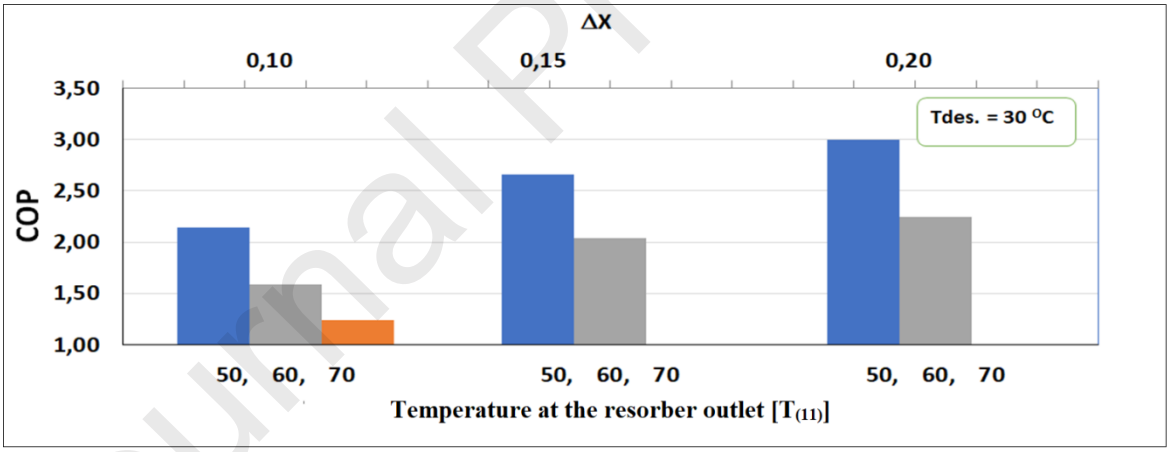

a)

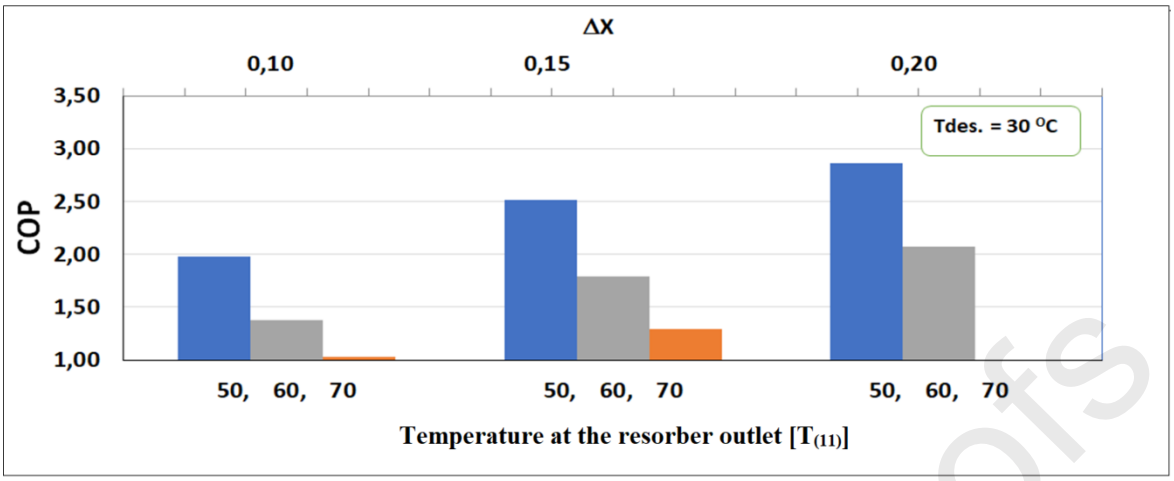

b)

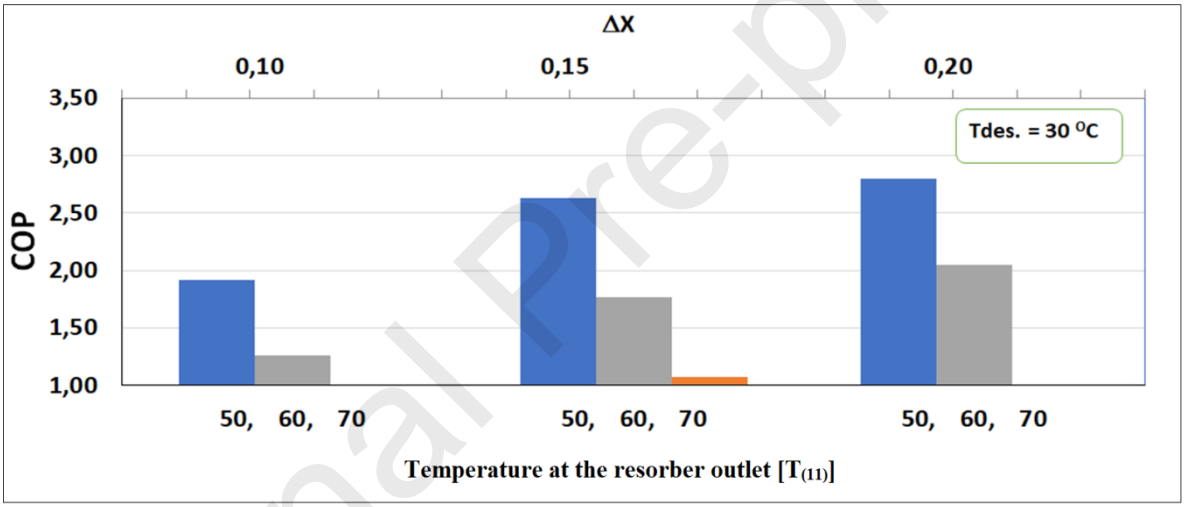

c)

Figure A 1. *The temperature at resorber outlet is between 50 ºC and 70ºC; The temperature at desorber is 30 ºC and the high pressure is of a)30 b)40 and c)50 bars*

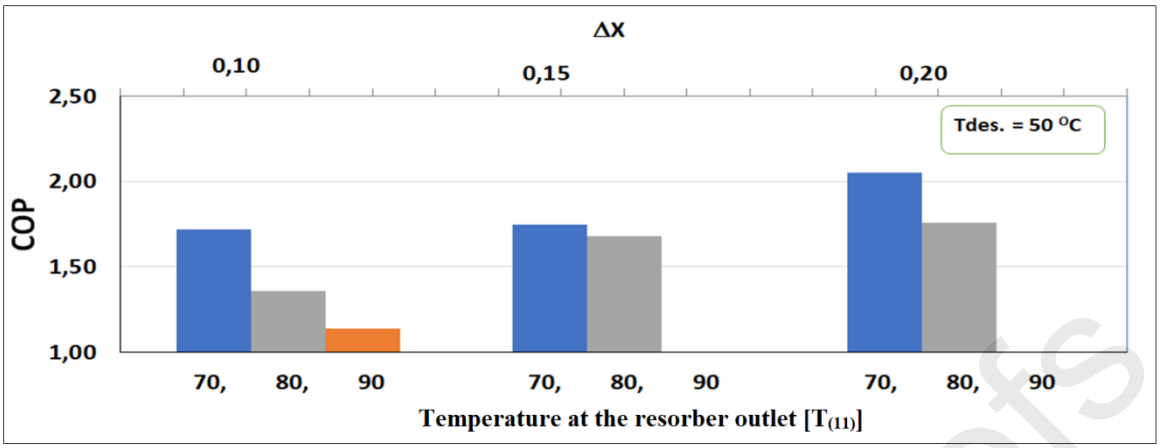

a)

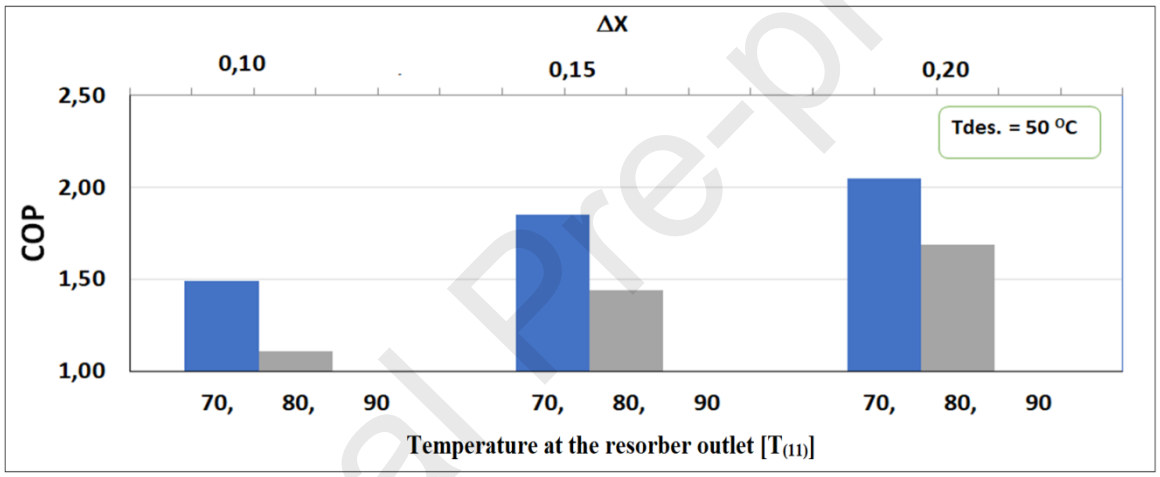

b)

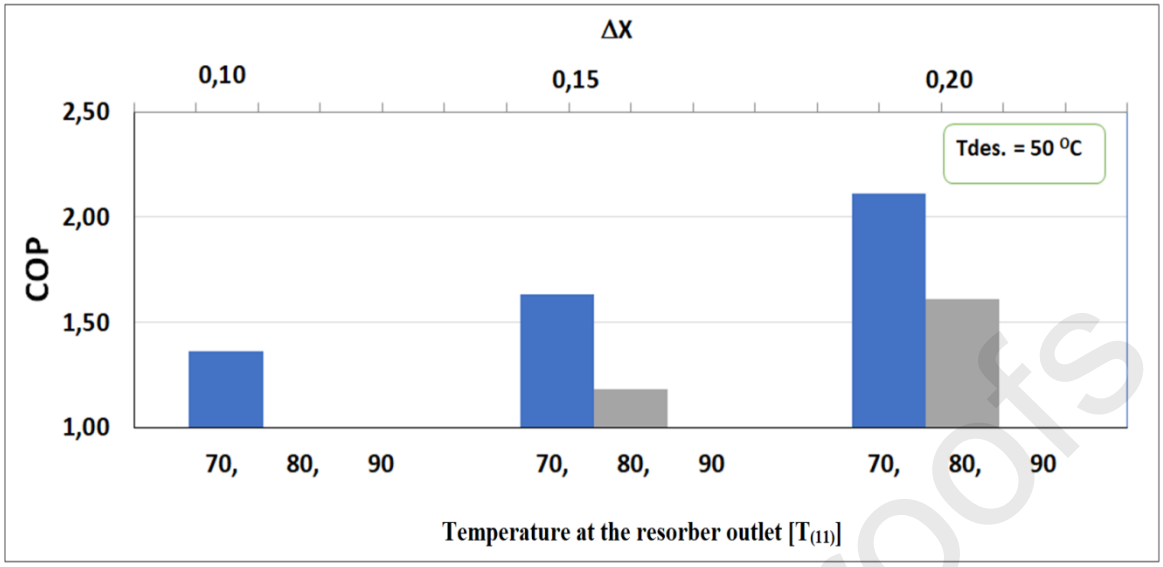

c)

Figure A 2. *The temperature at resorber outlet is between 70 ℃ and 90℃; The temperature at the desorber is 50 ℃ and the high pressure is of a)30 b)40 and 50 bars*

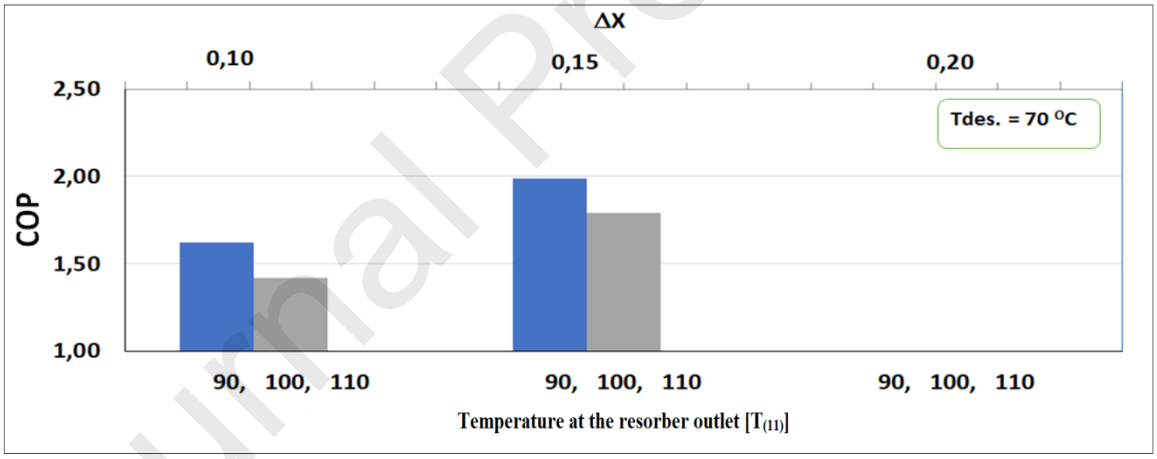

a)

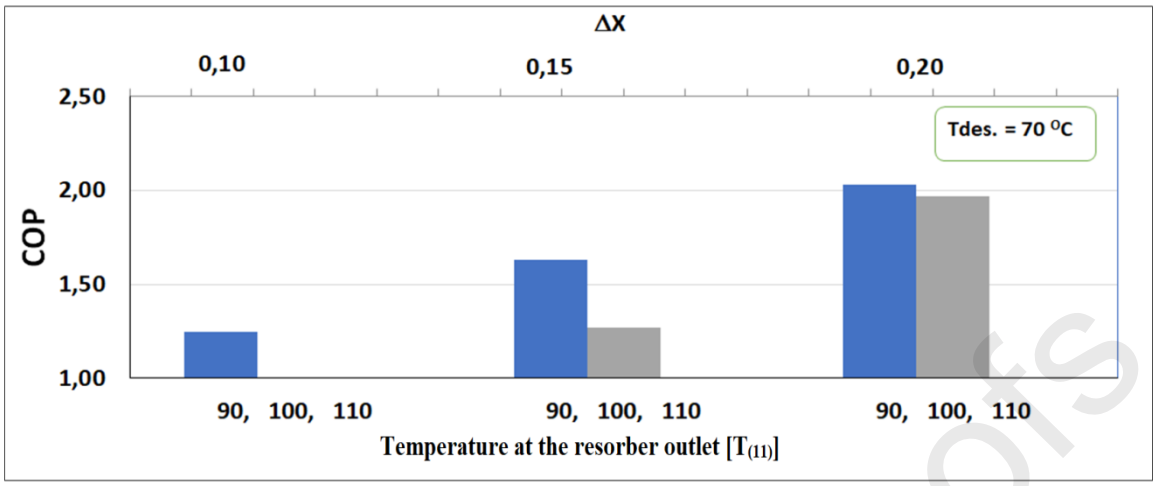

b)

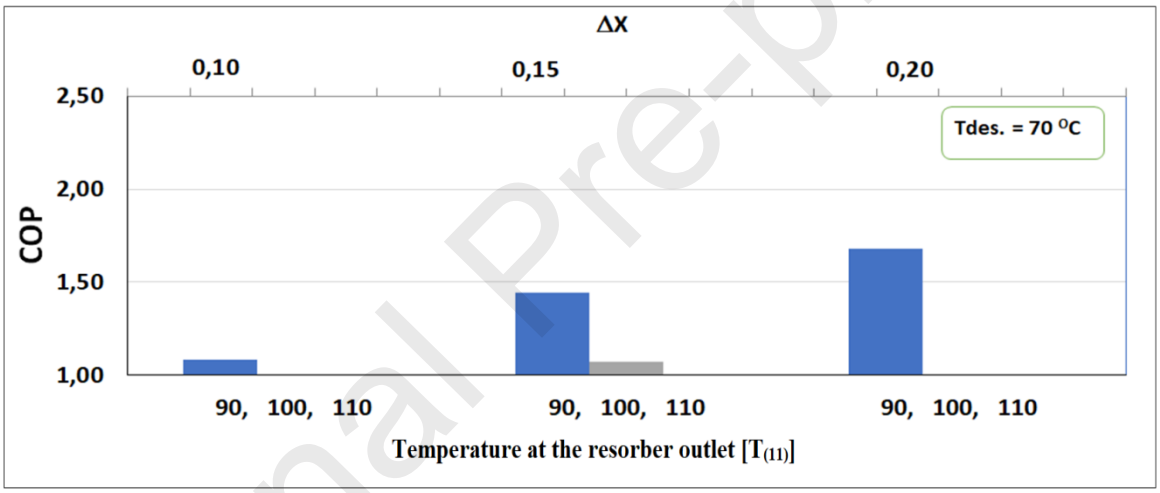

c)

Figure A 3. *The temperature at resorber outlet is between 90°C to 110; The temperature at desorber is 70 °C and the high pressure is of a)30 b)40 and 50 bars*

2. Appendix B

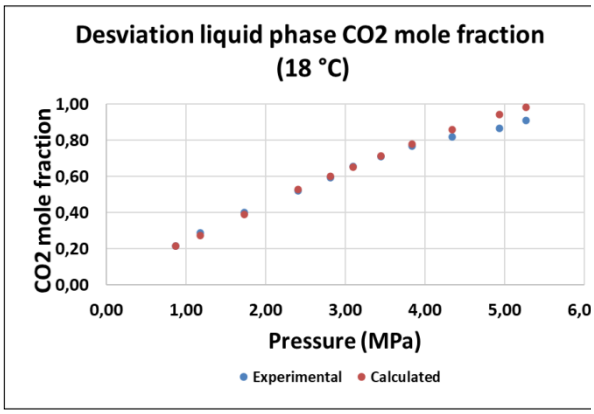

a)

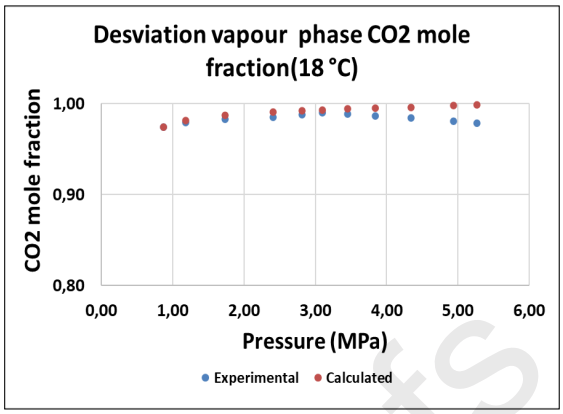

b)

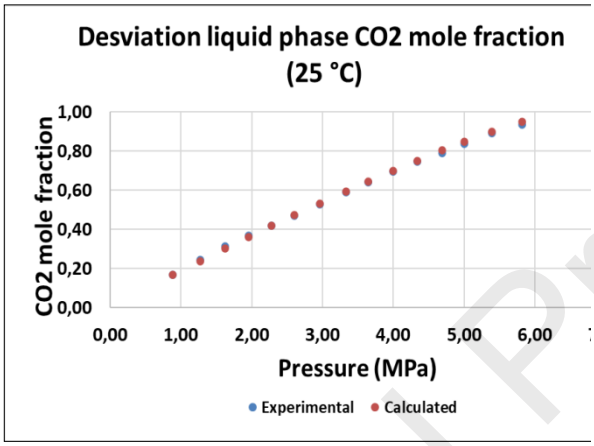

c)

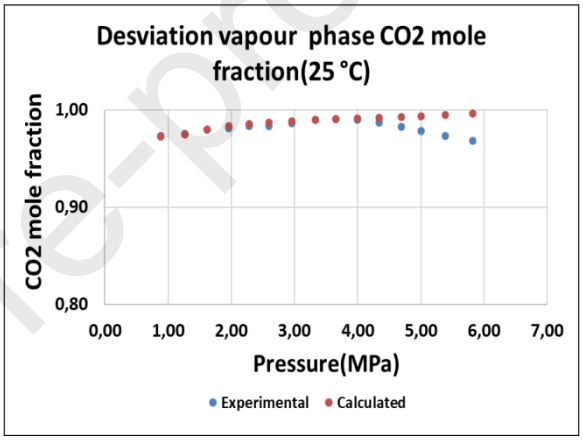

d)

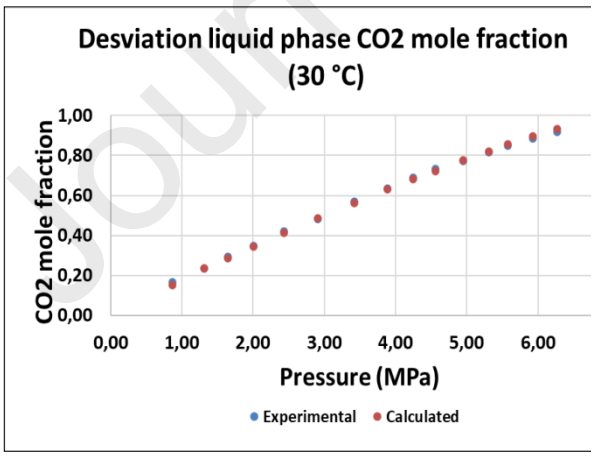

e)

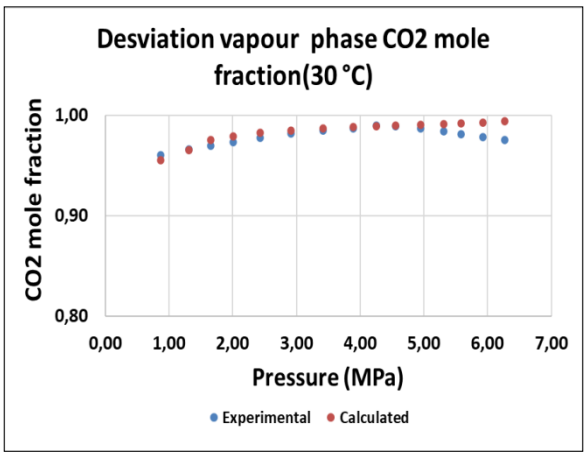

f)

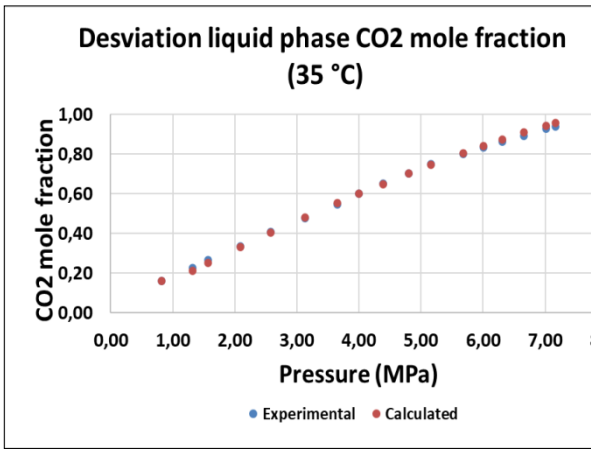

g)

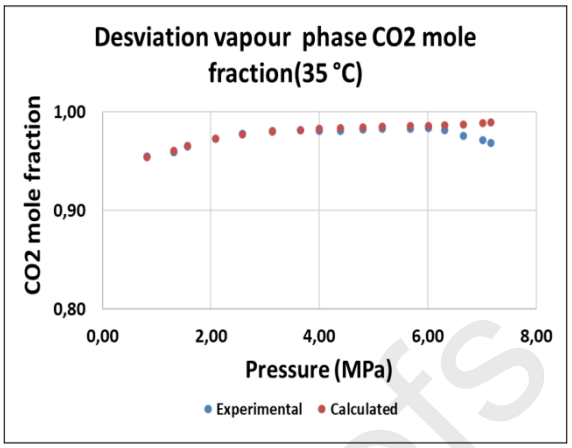

h)

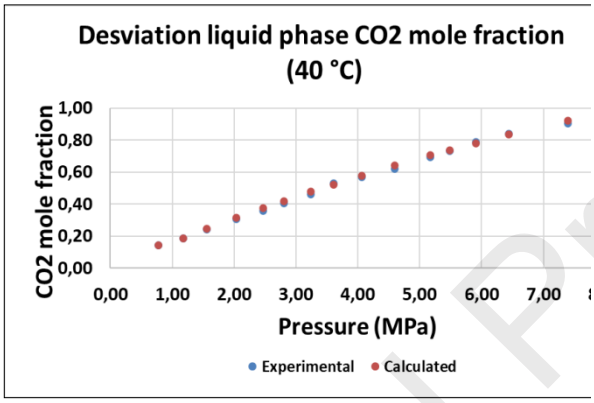

i)

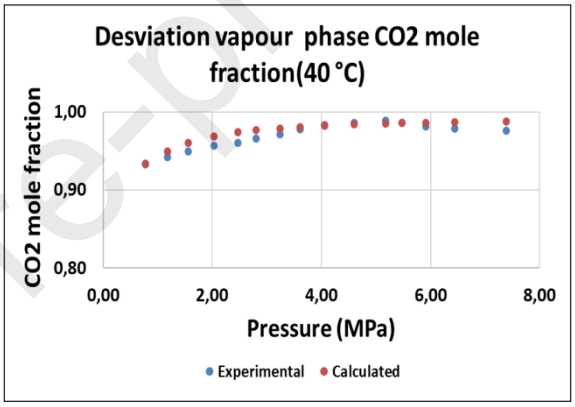

j)

Figure B 1. Comparison of data obtained with experimental data by Hsieh & Vrabec [40] of CO2 mass fraction deviation in liquid phase at **a)** 18 ˚C **c)** 25 ˚C **e)** 30 ˚C **g)** 35 ˚C **i)** 40 ˚C and vapour phase at **b)** 18 ˚C **d)** 25 ˚C **f)** 30 ˚C **h)** 35 ˚C **j)** 40 ˚C of CO2/acetone mixture.

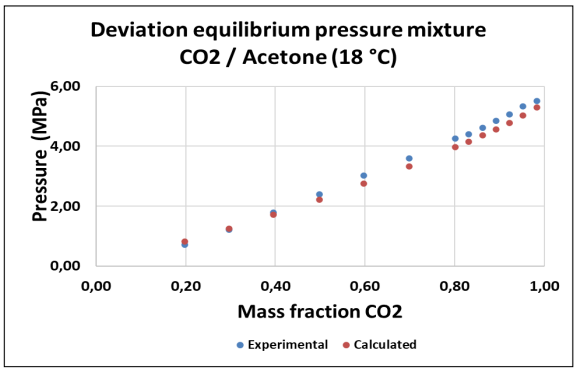

a)

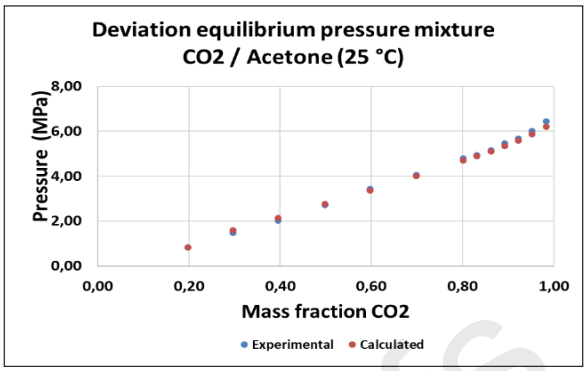

b)

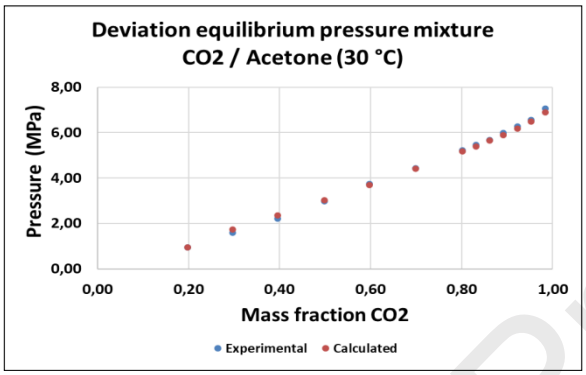

c)

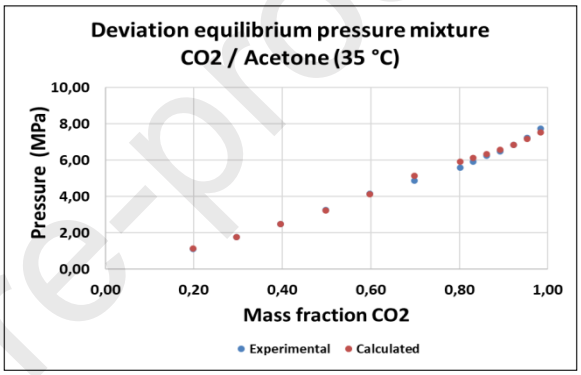

d)

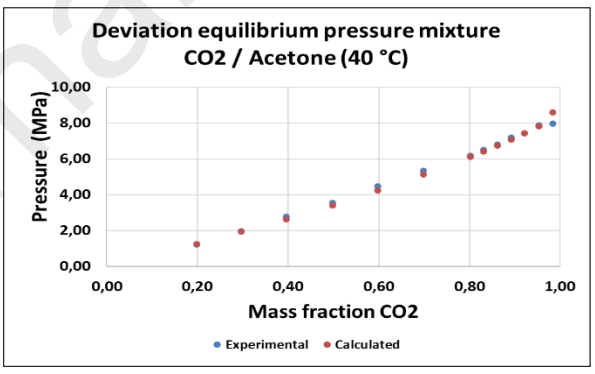

e)

Figure B 2. Comparison of data obtained with experimental data by Chiu et al., [41] of CO2 mass fraction deviation equilibrium pressure in liquid and vapor phase of CO2/acetone mixture at **a)** 18 ˚C **b)** 25 ˚C **c)** 30 ˚C **d)** 35 ˚C **e)** 40 ˚C

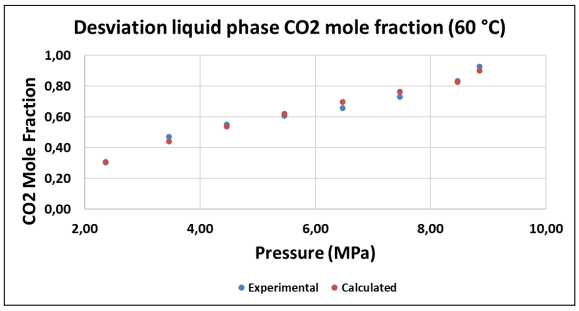

a)

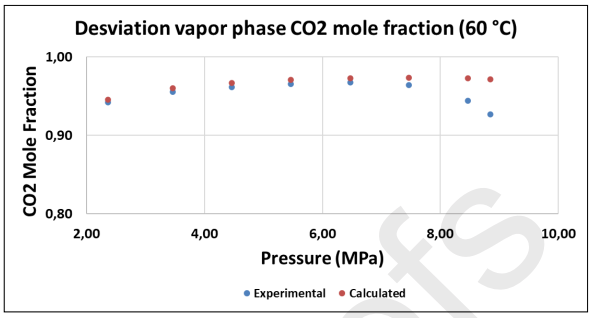

b)

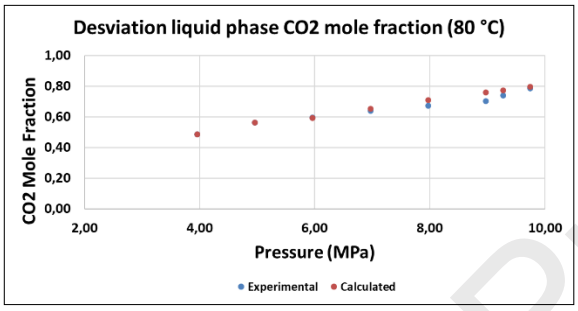

c)

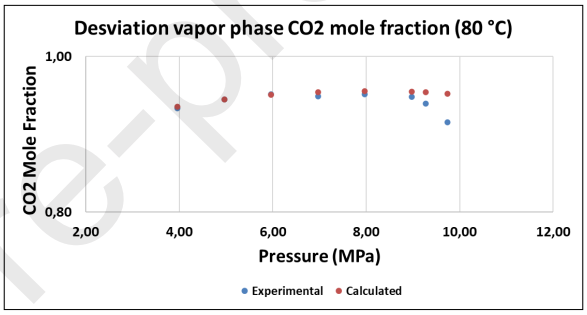

d)

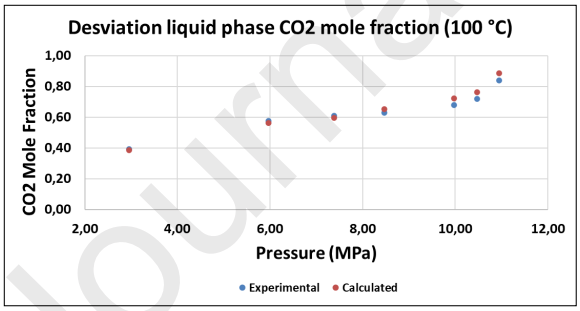

e)

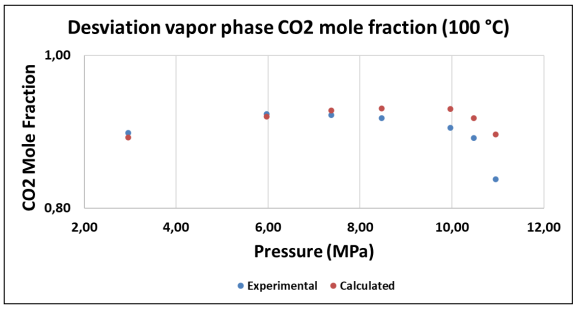

f)

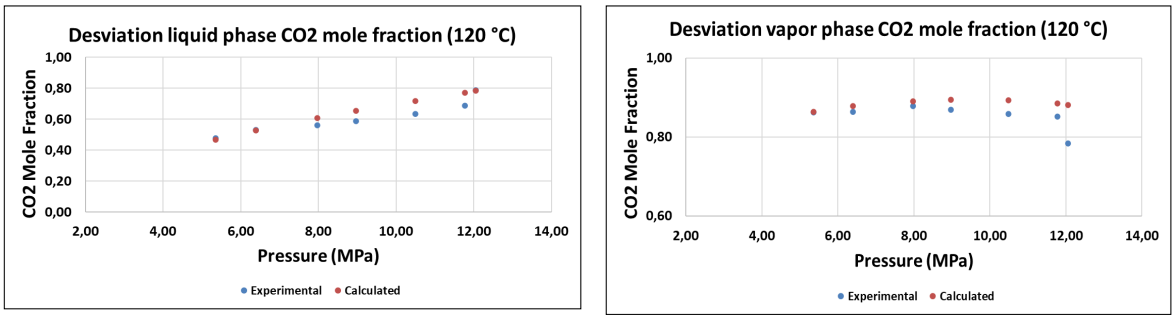

g) **h)**

Figure B 3. Comparison of data obtained with experimental data by Han et al., [39] of CO_2 mass fraction in liquid phase at **a)** 60 ˚C **c)** 80 ˚C **e)** 100 ˚C **g)** 120 ˚C and vapour phase at **b)** 60 ˚C **d)** 80 ˚C **f)** 100 ˚C **h)** 120 ˚C of CO2/acetone mixture.

Highlights

• Modelling of a CRHP with a acetone/CO2 mixture

• Application of Peng-Robinson equation for zeotropic mixture

• Calculation of thermal equilibria regarding pressure, temperature, and fluid concentration

• Analysis of the coefficient of performance for industrial conditions

Declaration of interests

☐ The authors declare that they have no known competing financial interests or personal relationships that could have appeared to influence the work reported in this paper.

☒The authors declare the following financial interests/personal relationships which may be considered as potential competing interests:

- Coronas, Alberto
- Bruno, Joan Carles
- Barba, M. Isabel
- Berdasco, Miguel
- Salavera, Daniel
- Larrechi, M. Soledad
- Valles, Manél